

ORACLES Final Report

Noah Brenner, Patrick Holstine, Matthew Kerner, Ioannis Loukidis, Rohan Ravikanti, David Reynolds, Aaron Trinh,
and Ethan Traub
Georgia Institute of Technology, Atlanta, GA, 30332

Contents

I Introduction	4
II Science Mission	4
II.A Science Goals	5
II.B Science Traceability Matrix	5
II.C Instrumentation	7
II.C.1 Orbiter Instruments	7
II.C.2 Lander Instruments	8
II.D Scientific Impact	9
III Concept of Operations	10
III.A Mission Timeline	11
IV Requirements Definition and Compliance Matrix	11
V Design Integration and Operation	13
V.A Launch, Trajectory, EDL	13
V.A.1 Launch, Trajectory, Requirements	13
V.A.2 Trajectory Analysis/Simulations	14
V.A.3 Aerobraking Maneuvers	16
V.A.4 EDL Analysis/Simulations	17
V.B Structures	22
V.B.1 Structures Requirements	22
V.B.2 GALE Structures	23
V.B.3 GALE Configuration and Mechanisms	25
V.B.4 AEGIS Structure, Configuration, and Mechanisms	27
V.B.5 Launch Vehicle Adapter	29
V.B.6 Operational Modes	29

V.C	Electric Power System	31
V.C.1	EPS Requirements	31
V.C.2	GALE	31
V.C.3	Entry, Descent, and Landing	33
V.C.4	AEGIS Lander	34
V.D	Propulsion System	36
V.D.1	Propulsion Requirements	37
V.D.2	GALE	37
V.D.3	AEGIS	38
V.E	Thermal Control System	40
V.E.1	TCS Requirements	40
V.E.2	EDL	41
V.E.3	GALE	42
V.E.4	AEGIS	44
V.F	Attitude Control System	46
V.F.1	ACS Requirements	46
V.F.2	Instruments aboard GALE	48
V.F.3	Instruments aboard AEGIS	48
V.F.4	Desaturation Analysis	49
V.F.5	Maximum Spacecraft Slew Rate Analysis	50
V.F.6	Pointing Jitter and Accuracy Estimation	51
V.G	Communications	52
V.G.1	Communications Requirements	52
V.G.2	AEGIS to GALE	53
V.G.3	GALE to Earth	54
V.G.4	Data Budget	55
VI	Mission Summary	57
VI.A	Cost Breakdown & Mass Budget	57
VI.B	Risk Analysis	58
VI.B.1	EDL Analysis	60
VI.B.2	Orbit Analysis	61
VI.B.3	Orbiter Instrument Analysis	61

VI.B.4 Lander Instrument Analysis	62
VI.B.5 Thermal System Analysis	62
VI.B.6 Power System Analysis	62
VI.B.7 Communication System Analysis	63
VI.B.8 Propulsion System Analysis	63
VI.B.9 ACS System Analysis	63
VI.C Scheduling	64
VII Conclusion	65
A Complete Requirements List	66
I Orbital Requirements	66
II Structures and Configuration Requirements	67
III Power Requirements	70
IV Propulsion System Requirements	71
V Thermal Requirements	72
VI Attitude Control System Requirements	73
VII Communications Requirements	75
VIII Payloads Requirements	76

I. Introduction

To prepare for human exploration of Mars, several questions still remain about Martian geological processes and atmospheric characteristics. The ORACLES mission aims to answer some of these questions through a two-pronged approach. By sending two spacecraft to the Red Planet, an orbiter in a polar science orbit paired with a lander targeting Hellas Planitia, the ORACLES mission (Orbital Reconnaissance and Aeolian Characterization with Landing Environmental Surveyor) will allow for near total coverage of the Martian surface as well as detailed in situ data in an area of interest suitable for human exploration. The orbiting spacecraft, GALE (Global Aeolian and Lithospheric Explorer), will provide data to improve models of Martian atmospheric weather and identify locations of subsurface resources. Meanwhile, the lander AEGIS (Atmospheric, Environmental, and Geological Investigation Station), will collect surface data regarding weather events occurring in Hellas Planitia, a site of frequent weather activity due to its lower elevation and therefore higher surface pressure. Launching in December 2028 and completing the primary mission by the end of 2033, the ORACLES mission will advance the understanding of the evolution of planetary atmospheres and increase the safety of future manned missions through a more complete understanding of Martian weather.

II. Science Mission

In the NASA Moon to Mars document, several key areas of study in the 2023 Planetary Science Decadal Survey are outlined to prepare for human exploration of the Red Planet. Out of these areas of study, there is an emphasis on characterizing the martian atmosphere in detail, since many questions about its formation, aeolian processes, surface-atmosphere coupling, energy and momentum are unanswered. With this information, scientists could gain a better understanding of the Martian climate and geological processes, leading to improved models for predicting weather phenomena, particularly dust storms [1]. Continuous monitoring of the Martian atmosphere would enhance understanding of its dynamic interactions with the surface, enabling more accurate environmental modeling. This information is essential for designing robust entry, descent, and landing systems to ensure the safety and success of future human exploration missions.

Another scientific objective described in the Moon to Mars document is to locate and identify accessible in situ resources that would support human exploration of Mars. This includes materials that could be converted into fuel for spacecraft entering and exiting the Martian atmosphere, used as life support for human explorers, or used in other ways that would make Mars exploration sustainable. For example, this could include subsurface water ice deposits as well as areas or resources with radiation shielding capabilities. If mission planners have information on where these potential resources or natural formations may be and their approximate abundance, suitable areas of exploration could be identified, allowing explorers to utilize these resources during the course of their mission.

The overarching mission of ORACLES will be to answer questions for these two major scientific objectives, which will bring humanity significantly closer towards a crewed exploration mission to Mars.

A. Science Goals

The **ORACLES Mission** will tackle three main objectives which revolve around paving the way for the near-future human exploration of Mars:

- 1) Obtaining high-resolution winds and atmospheric dynamics data across at least 75% of the Martian surface over multiple annual cycles;
- 2) Detecting and monitoring the location and volume of subsurface water ice deposits, as well as potential solidified lava tubes over multiple annual cycles;
- 3) Collecting in-situ data on surface dust saltation and characterizing dust height versus particle size in Hellas Planitia, a promising landing spot for future human exploration.

To accomplish this scientific mission and achieve these objectives, ORACLES will consist of two spacecraft that will be launched together in one launch and cruise vehicle - **GALE** and **AEGIS**. GALE will be deployed as a multi-year orbiter in a sun-synchronous orbit around Mars, where it will utilize a suite of instruments to tackle objectives 1) and 2) listed above. AEGIS will be deployed as a lander, which will first follow a direct entry trajectory to the Martian surface, where it will collect high-resolution atmospheric composition and thermal/pressure profile data. This descent will end in a landing in Hellas Planitia, a 1400-kilometer wide, 8-kilometer deep basin, which is a prime spot for future human exploration due to its relatively higher air pressure and possible shallow water sources; however, these conditions make this basin prone to strong wind and dust storms. AEGIS is equipped with instruments that will tackle objective 3) as listed above, to provide improved data for surface erosion and dust storm models.

B. Science Traceability Matrix

The implementation of a Science Traceability Matrix (STM) is a common practice among NASA and ESA to explicitly define the scientific objectives driving the mission as well as instrument requirements necessary to achieve each objective. The STM for ORACLES outlines the overarching science goals guiding the mission, the specific science objectives derived from these goals, and the high-level measurement and instrumentation requirements needed to fulfill them. The ORACLES STM is presented below in table 1.

Science/Technology Goals	Science/Technology Objectives	Measurement Requirements		Instrument Requirements		Projected Performance	Mission Requirements (Top Level)
		Physical Parameters	Observables				
Understand the geological processes that affect Mars by characterizing the evolution of the atmosphere/exosphere and investigate how active processes modify the surface of Mars. Characterize the atmosphere and geology on the surface of Hellas Planitia to determine if its conditions and resources could support human exploration. Determine whether the higher pressure of the Martian crater Hellas Planitia creates changes in geological/atmospheric conditions influencing the wind dynamics on Mars.	Determine how atmospheric waves drive atmospheric dynamics and energetics through thermal and direct wind measurements over multiple annual cycles.	Wind vector maps of Mars' atmosphere as a function of surface altitude; atmospheric temperature/pressure data as a function of surface altitude.	Laser frequency doppler shift (due to atmospheric winds/particles)	Atmospheric vertical Resolution	300 meters	150 meters	Sun-synchronous orbit required to correctly analyze Doppler shifts and frequencies of light with respect to time/respect to an area of the Martian atmosphere. Laser doppler shifts and mie scattering help identify dust and aeolian activity.
		Degree of Mie scattering of dust particles		Column Height	Surface to 25km	Surface to 30 km	
		Thermal inertial and temperature profiles		Interferometer Resolution	90 MHz	100 MHz	
		Three-dimensional flux rate for transported sand and dust, grain sizes within transport layers; Graph of dust flux rate versus grain size for varying heights	Infrared emission spectra	Spatial/Spectral Resolution	50m/pixel, 330-410nm at 6 nm/channel	15-19m/pixel, 362-395nm at 6.55 nm/channel	Thermal inertial mapping/profiling required for building high fidelity atmospheric wind profiles.
		Size, height, and velocity of saltating dust and sand grains; Probability distribution graph of grain size versus probability of saltation		Frequency of scattered light	Wind Speed Range	0-100 m/s	0-100 m/s
	Investigate composition and cause of variability in Martian dust storms. Identify geological/atmospheric resources existing in the Martian boundary layer and in Hellas Planitia that could facilitate human exploration on Mars.	Imaging during descent	Black and white images	Sampling Frequency	8 frames per second	15 frames per 1.5 seconds	
		Body static pressure through entry and descent	Sensor Voltages	Maximum Operative Temperature	62 °C	90 °C	
		Body shell heat map	Infrared radiation	Maximum Operative Temperature	60 °C	75 °C	
		Body heat flux profiles through entry	Heat flux measured through temerpature difference	Maximum Operative Temperature	98 °C	200 °C	
		Depth/volume of ice/water deposits (via orbiter's ground penetrating radar)	Radar time of flight	Depth	1 km	5km	
Identify geological/atmospheric resources existing in the Martian boundary layer and in Hellas Planitia that could facilitate human exploration on Mars.	Identify geological/atmospheric resources existing in the Martian boundary layer and in Hellas Planitia that could facilitate human exploration on Mars.	Sediment deposits	Images of data-collection areas	Range Resolution	5mm at 2m range	1mm at 2m range	
		Aerosol backscattering profiles	Semiconductor laser pulses	Spatial Resolution	15-30m	7.5-15m	
		Surface radiation exposure	Differential energy fluxes	LET Range	1-800 keV/μm	0.2-1000 keV/μm	
		Surface temperature	Sensor voltages	Temperature Resolution	0.05 K	0.04 K	
		Surface pressure	Sensor voltages	Pressure Resolution	0.5 Pa	0.5 Pa	
		Surface humidity	Sensor voltages	Humidity Resolution	0.50%	0.50%	
		Wind speed and direction	Sensor voltages	Velocity Range	1 - 30 m/s	0.3 - 30 m/s	
		Local atmospheric potential	Sensor voltages	Potential Range	-10, +10 V	-10, +10 V	
		Intensity of solar radiation	Sensor voltages	Irradiance Resolution	10^-4 W/m^2	3.7*10^-4 W/m^2	
		Three body-axes accelerations	Sensor voltages	Acceleration Range	0.1 mm/s^2 - 200 m/s^2	10 μm/s^2 - 200 m/s^2	
				Acceleration Accuracy	0.10%	0.082%	

Fig. 1 Science Traceability Matrix

In accordance with our Mission Statement, our three primary objectives are to investigate the dynamics of the Martian atmosphere, the composition and cause of Martian dust storms, and the viability of Hellas Planitia as a location for human habitation. Early research has given us a scope of the available and appropriate instrumentation for each objective and an idea of systems that may be less mission-critical but easily implementable and nonetheless significant for broader planetary science.

To maximize coverage of the Martian atmosphere, GALE will use its high altitude to obtain relatively lower resolution measurements but will also employ novel technology to accurately characterize the Martian boundary layer and its aeolian dynamics. The first objective is addressed principally through GALE's operations in obtaining various emission spectra, Doppler-shifted frequencies, and thermal profiling outlined in Figure 2. AEGIS will focus on minute and highly accurate in situ point data along its trajectory and in Hellas Planitia, our labeled location of interest. The onboard suite of aerothermal sensors, developed specifically for data-collection during the hypersonic phase of reentry, will take advantage of the journey to the surface to cross-validate orbiter data on the gas composition and state through the high atmosphere, boundary layer, and crater descent. On landing, AEGIS will employ its surface laboratory to characterize the local environment in Hellas Planitia. Dust dynamics in the crater and elsewhere will be investigated

from GALE with thermal inertial maps and scattering analysis. On the surface and within the crater, AEGIS will focus on mesoscopic dust dynamics and saltation and will make use of an electrostatic probe to quantify the electric potential at the surface and its effects on dust activity and the formation of dust storms.

C. Instrumentation

1. Orbiter Instruments

In the orbiter instrument suite, the primary instrument for the ORACLES mission will be a space-grade version of NASA's Doppler Aerosol Wind Lidar (DAWN), selected for its exceptional capability to provide high-resolution wind and dust data on Mars. This capability is supported by the extensive dataset generated by the AEOLUS mission, which has significantly enhanced the understanding of Earth aeolian processes [2]. While previous missions have employed spectrometers and other instruments to analyze Martian wind patterns, DAWN will be the first to directly measure aeolian activity and dust dynamics using laser frequency Doppler shifts. With this approach, wind vector maps and mie scattering of dust particles can be directly obtained, offering a wealth of data to characterize the martian atmosphere with. In doing so, DAWN will directly contribute to the first scientific objective outlined in the STM and the first scientific goal of the ORACLES mission. Furthermore, its integration with other instruments from the ORACLES mission will reinforce and validate the collected data, enhancing overall scientific outcomes.

An imaging spectrometer similar to the Compact Reconnaissance Imaging Spectrometer for Mars (CRISM) onboard the Mars Reconnaissance Orbiter (MRO) was also selected to be onboard the GALE orbiter. Having an infrared spectrometer would be an ideal complement to the wind Doppler lidar, serving as a valuable tool for verifying wind and dust observations, as well as strengthening the database of wind data that scientists will rely on to characterize Martian aeolian activity. This pairing is supported by a well-established correlation between wind activity in an atmosphere and the distribution of temperature and pressure within that atmosphere [3]. Moreover, while CRISM's primary objective is to analyze surface mineralogy, its use in the context of the ORACLES mission would be as a dedicated atmospheric instrument.

To enhance thermal inertia profiling and support DAWN observations, the Mars Climate Sounder (MCS) has been selected to measure thermal distributions across various altitudes in Mars' atmosphere. The decision to include the Mars Climate Sounder (MCS) onboard GALE is based on its proven performance on previous missions, such as Mars Express, where it successfully provided valuable atmospheric data. Additionally, co-locating MCS with the wind lidar and imaging spectrometer enables simultaneous observations of the same atmospheric region, allowing for more comprehensive data collection and cross-validation between instruments. This integrated configuration allows GALE to produce a high-resolution, multi-dimensional atmospheric dataset with built-in redundancies, minimizing measurement uncertainties and significantly increasing the volume and reliability of data.

Finally, a subsurface radar sounder was selected onboard GALE to investigate subsurface resources within Hellas

Planitia, directly supporting the mission's second science goal and the third scientific objective outlined in the STM. A ground-penetrating radar like the Mars Advanced Radar for Subsurface and Ionospheric Sounding (MARSIS) radar onboard Mars Express is ideally suited for detecting subsurface water ice and potential lava tubes that could offer natural radiation shielding, which are two critical resources for human exploration on Mars. Given the success of the radar sounder on Mars Express and the lack of any other Mars-orbiting instruments dedicated to subsurface analysis in Hellas Planitia, this instrument is arguably the best choice to study the crater's composition. Additionally, since many of the science instruments onboard GALE are dedicated to studying the Martian atmosphere, having an orbiter instrument dedicated to resource analysis on Mars will complement the instruments selected for resource analysis on AEGIS.

2. Lander Instruments

In order to collect *in situ* data on Martian aeolian transport, AEGIS has been equipped with a saltation sensor and a dust anemometer. Together, these instruments will analyze the movement of sedimentary particles and dust on the surface of Mars and in the low atmosphere, which has direct correlations to wind activity. The intensity and variability of wind activity will be inferred from the motion of particles of different grain sizes detected by the saltation sensor, as well as the velocity of dust particles measured by the dust anemometer. Since AEGIS is in Hellas Planitia, a place of high wind activity due to higher surface pressures, the data from these sensors will be excellent tools for understanding the origin of aeolian activity, helping further to model the Martian atmosphere. This supports GALE in the first science goal of ORACLES and directly addresses the third science goal for the mission.

Another objective that AEGIS will achieve on the surface of Hellas Planitia will be to characterize the electric phenomena that occurs in the Martian atmosphere, as part of the effort to produce a full atmospheric model for future exploration missions. An electric field sensor and flux radiometer have been equipped in the science instrument suite, where they will assess the distribution of electricity and radiation on the surface. With this data, scientists will have more information to understand the origin of storms that form on Mars and potentially plan around it. Additionally, the flux radiometer will provide information of the solar irradiance inside Hellas Planitia, which will help future exploration missions going to Hellas Planitia develop successful electric power system solutions.

To further describe the surface conditions on the surface of Mars in Hellas Planitia, thermopiles, pressure transducers, 2D wind sensors, radiation detectors, and imaging cameras have all been included on AEGIS. Thermopiles will monitor surface temperature fluctuations throughout the sol, while pressure transducers will track atmospheric pressure changes to support the study of Martian weather patterns. The 2D wind sensors will characterize wind direction and speed, providing supporting data in conjunction with the saltation sensor and dust anemometer for understanding aeolian processes and dust transport. Radiation detectors will assess radiation levels in the crater surface, which will help determine if areas in particular within Hellas Planitia are lower in radiation content. Finally, imaging cameras will visually document the terrain and environmental conditions, offering context to dust saltation measurements and

supporting geological assessments of Hellas Planitia.

During the entry, descent, and landing (EDL) phase, AEGIS is equipped with a radar Doppler altimeter, an aerothermal sensor suite, and descent cameras to document the descent in the Martian atmosphere. The radar Doppler altimeter will provide real-time measurements of altitude relative to the ground, which will enable the aerothermal sensor suite to collect a full profile of in situ atmospheric data throughout the entire descent to the surface. The aerothermal sensor suite, which consists of multiple thermocouples, pressure transducers and recession sensors to document the aerothermal environment during descent, as well as aerodynamic and atmospheric activity during descent. Complementing these instruments, the descent cameras will record high-resolution imagery of the terrain and spacecraft throughout descent, which will be useful should future spacecraft explore Hellas Planitia. By directly measuring temperature, pressure, and material recession during descent, the aerothermal sensor suite will provide a complete in situ atmospheric profile during descent, which will be supporting atmospheric data collected by both GALE and AEGIS. Additionally, reconstructing the trajectory from the AEGIS lander will improve design margins for future Mars entry and descent to Hellas Planitia, enabling a well informed entry profile for future exploration missions to the crater.

D. Scientific Impact

Precise characterization of the Martian atmosphere is a critical prerequisite for the design and optimization of entry, descent, and landing (EDL) systems for future crewed missions. This mission will provide vertically and spatially resolved data on atmospheric density, composition, pressure, and temperature across diurnal, seasonal, and regional variations. These datasets will directly reduce modeling uncertainties in atmospheric entry simulations, enabling more accurate prediction of aerodynamic forces and thermal loads. Improved fidelity in EDL design parameters will permit narrower landing ellipses and more reliable surface access, both of which are essential for mission safety and logistical planning for any exploration mission to the Martian surface.

Simultaneously, this mission will employ remote sensing and in situ analysis to identify and quantify accessible surface and subsurface resources, with particular emphasis on water ice, hydrated regolith, and potential natural shelters such as lava tubes. Lava tubes provide a natural means of radiation shielding, protecting astronauts from harmful cosmic and solar radiation, a critical concern for long-duration missions. The mission will assess the location, size, and accessibility of these lava tubes to determine their viability as sites for habitats or storage, significantly enhancing the safety and sustainability of human missions. In addition, geological and atmospheric constituents relevant to in-situ resource utilization (ISRU) will be analyzed, contributing to strategies for producing water, oxygen, and other life support materials locally, thus reducing reliance on Earth-based resupply.

Together, these two major investigative threads—atmospheric profiling and resource prospecting—form the scientific backbone necessary for a transition from reconnaissance to sustained human presence. By generating high-resolution environmental and resource datasets, this mission will close knowledge gaps in EDL system engineering and ISRU

infrastructure design. The resulting models and maps will be foundational to future mission architectures, informing the placement of habitats, power systems, and life-support infrastructure, and ultimately enabling the development of self-sufficient outposts on Mars.

III. Concept of Operations

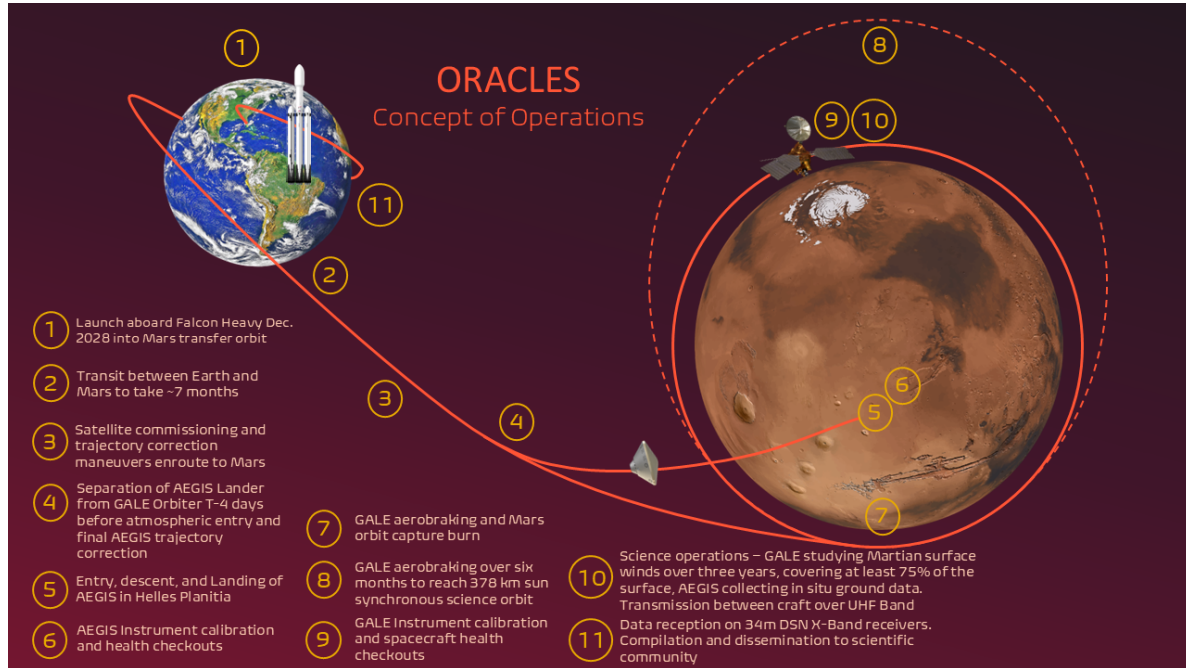


Fig. 2 Concept of Operations for ORACLES

The concept of operations describes how the mission will operate. For the ORACLES mission, the spacecraft will launch atop a Falcon Heavy spacecraft during the December 2028 transfer window. The transfer to Mars will take approximately seven months, which is typical for most Mars missions using a type-1 orbital transfer.

During the journey to Mars, the spacecraft will undergo commissioning of its subsystems and perform a series of correction burns to ensure the AEGIS lander will land in Hellas Planitia and the GALE orbiter is on an aerobraking approach. On approach to Mars, at T-4 days, the AEGIS lander will disconnect from the GALE orbiter, and perform one final correction burn to target Hellas Planitia. The lander will descend into the Martian atmosphere on a trajectory to Hellas Planitia, while the orbiter will use its propulsion system and the upper Martian atmosphere to capture into an eccentric orbit. Once landed, the AEGIS lander begins all instrument calibration and health checkouts in preparation for science observations.

Over the course of six months, the orbiter will use the upper Martian atmosphere to shrink its orbit to a 378 km Sun synchronous polar orbit when the propulsion system will again be used to raise the periapsis and circularize the orbit. In this science orbit, the GALE craft begins calibrating all instruments onboard and performing health checkouts to ensure

no damage during aerobraking and propulsive maneuvers. Over the next 3 years, the GALE orbiter will collect data to generate a map of Martian winds over at least 75% of the Martian surface while the AEGIS lander collects in situ ground data of weather and surface dust properties. The spacecraft will communicate between each other using UHF band transceivers and the GALE craft is capable of transmitting to Earth using X-band frequencies on 34m Deep Space Network antennas where data can then be compiled and disseminated to the broader scientific community and general public for use in planning future manned Mars missions.

A. Mission Timeline

IV. Requirements Definition and Compliance Matrix

The formal requirements nomenclature for the ORACLES mission is as follows: for top-level, parent requirements, these are comprised of three components separated by dashes - the first component is comprised of two letters and refers to the vehicle at hand - either "GA" for GALE, "AE" for AEGIS, or "OR" for requirements that apply to both vehicles. The second component refers to the relevant subsystem on the vehicle at hand and is comprised of three to five letters - for example, orbital requirements are listed as "ORB," attitude requirements are listed as "ACS," payloads requirements are listed as "INSTR," etc. The third component is the requirement number/ID. Child requirements are listed as the parent requirement ID appended with ".XX" (two digits) corresponding to the child requirement ID.

Here is an example for clarity: the first child requirement of the first top-level requirement in the power subsystem of AEGIS would be listed as: "AE-POW-01.01."

Mission and system requirements can be found in Table 1, more requirements for individual subsystems are available in the appendix VII.

Table 1 Requirements and Compliance Matrix

ID	Requirement	Compliance Criteria
MIS-OR-01	The total cost of the mission shall not exceed \$1 billion	Budget reports, financial audits, cost breakdown in section VI.A
MIS-OR-02	The primary mission shall conclude no later than Dec. 31, 2033	Project timeline in section \ref{schedule}, mission completion reports
MIS-OR-03	The primary mission shall provide data encompassing coverage of least 75% of the Martian globe	Data collection reports, coverage maps, orbit design in section V.A
MIS-OR-04	The primary mission shall collect data over multiple annual cycles	Data collection schedules, mission logs, planned mission timeline in section VI.C
MIS-OR-05	The mission shall launch no later than December 31, 2028	Launch schedule, mission timeline, planned mission timeline in section VI.C
MIS-OR-06	Each spacecraft bus shall enable the survival of both spacecraft during launch, transfer, and operations	Engineering reports, ground vibration testing, ground day in the life testing
MIS-OR-07	Each spacecraft shall be able to communicate while in transfer to Mars and during nominal operations when having line of sight with Earth	Communication logs, system tests, communications system design in section V.G
SYS-OR-01	The lander shall collect data on atmospheric winds via laser doppler velocimetry	Data collection reports, instrument specifications outlined in section II.C
SYS-OR-02	The lander shall collect data on grain sizes of dust uplifted via saltation	Data collection reports, instrument specifications outlined in section II.C
SYS-OR-03	The orbiter shall look for water ice and lava tubes providing natural radiation inside Hellas Planitia	Data collection reports, instrument specifications outlined in section II.C
SYS-OR-04	The orbiter shall collect atmospheric wind and dust data of the entire Martian atmosphere	Data collection reports, instrument specifications outlined in section II.C
SYS-OR-05	The lander and orbiter shall both weigh less than 2000kg each	Weight verification reports, engineering specifications, mass budget outlined in section VI.A
SYS-OR-06	The lander and orbiter shall fit within a 13.1m tall and 5.2m diameter fairing	Engineering specifications, fit tests, structural design specifications in section V.B
SYS-OR-07	The lander and orbiter shall provide approximately 118 W and 1270 W of operational power, respectively, to ensure consistent investigation and usage of scientific instruments, data handling, and communication systems	Power verification reports, system tests, power system specifications outlined in section V.C
SYS-OR-08	The orbiter and lander shall have a maximum interior dimension of (2.05m x 1.85m x 1.60m) and (1.55m \varnothing x 0.475m thickness) respectively	Engineering specifications, fit tests, structural design specifications in section V.B

V. Design Integration and Operation

A. Launch, Trajectory, EDL

1. Launch, Trajectory, Requirements

The ORACLES mission is planned to launch on December 31, 2028 on top of a falcon heavy launch vehicle. The falcon heavy was chosen for two main reasons. The cost was low compared to some of the other options and it has enough delta v to put the ORACLES spacecraft on a trajectory to Mars. The transfer date from earth to mars was chosen using the NASA Ames Research Center Trajectory Browser. This date was chosen for it's minimal Δv expenditure and fast transit time to Mars of 224 Days.

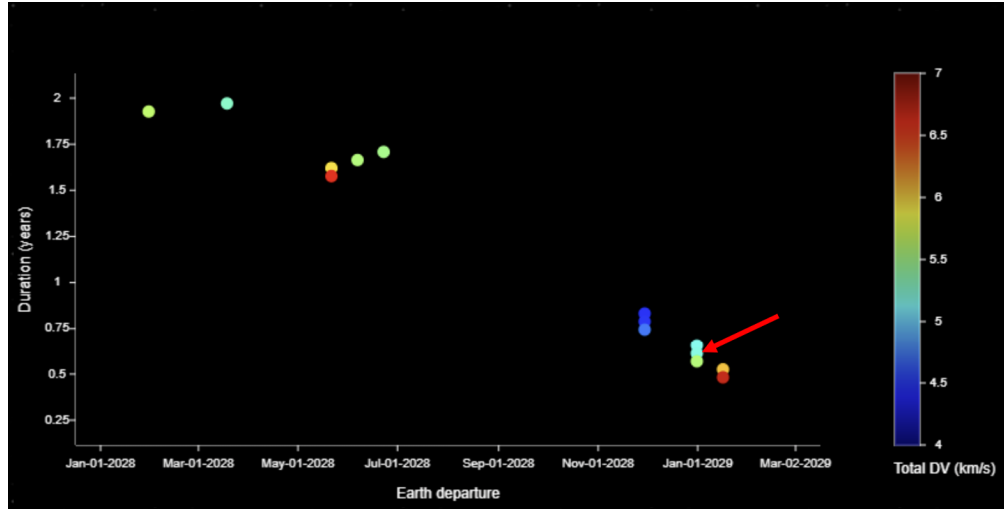


Fig. 3 Possible launch dates and the associated Δv with chosen launch date on December 31, 2028 and Δv of 3.8km/s. Courtesy of NASA Ames Trajectory Browser [4]

The requirements for the Launch, Trajectory and EDL are responsible to crafting a safe way to get the orbiter and lander to their desired orbit and location on Mars. Furthermore there are science requirements for the orbiter such as getting 75% coverage of the planet. This drives the science requirement to be in a sun-synchronous orbit. Also the Aegis lander science requirements drive that the lander must landing in Hellas Planitia as shown in table 2.

Table 2 Trajectory Requirements

ID	Requirement	Rationale
GA-ORB-01	Delta-V usage of GALE shall be less than then 2 km/s.	Increase fuel and therefore operational life-time of the mission.
GA-ORB-02	The GALE spacecraft must be in a Martian sun-synchronous 378 km orbit by January 1st 2031.	This is to allow for the gathering of science data by 2033 and the spacecraft should be able to maintain 75% orbital coverage.
GA-ORB-03	The GALE spacecraft periapsis shall be between 100 km and 120 km for aerobraking to lower its orbit.	This is to comply with requirement GA-ORB-01 to minimize delta v usage.
GA-ORB-04	The orbiter shall separate from the lander four days before before the Mars capture burn.	This is to comply with requirement GA-ORB-01 to minimize delta v usage.
AE-ORB-01	Lander shall land in Hellas Planitia located within a 100 km radius of 42.4° South latitude and 70.5° East longitude.	This is a science requirement.
AE-ORB-02	During Entry Decent and Landing AEGIS utilize a direct descent trajectory where the periapsis must be below 20 km in altitude.	This is a functional requirement.
AE-ORB-03	Delta-V usage of AEGIS shall be less than then 1 km/s.	This is to comply with AE-ORB-01.

2. Trajectory Analysis/Simulations

Using NASA Ames Research Center Trajectory Browser gives an approximate Δv expenditure for transfer however it does not give fine control over the parameters such as initial and final orbit altitude. In our approach, this requirement is addressed by formulating and solving Lambert's problem numerically in MATLAB. Lambert's problem determines the orbital trajectory connecting two specified points in space within a given time interval. Specifically, the position vectors of Earth and Mars at their respective launch and arrival dates were accurately obtained using NASA's SPICE toolkit, providing the initial conditions necessary for the Lambert solution as shown in figure 4. The dates and Δv of each maneuver are shown in table 3.

Table 3 Table of Maneuver with Δv , burn vehicle and Epoch

Maneuvers	Epoch	Burn Vehicle	Nominal Delta V (km/s)
Earth Departure	December 31, 2028	Falcon Heavy 2nd Stage	3.797
Course Correction	TBD	GALE	0.050
Mars Arrival	August 12, 2029	GALE	1.541
Mars SSO circularization	January 9, 2030	GALE	0.060
Total Delta V			5.448
GALE Delta V			1.651

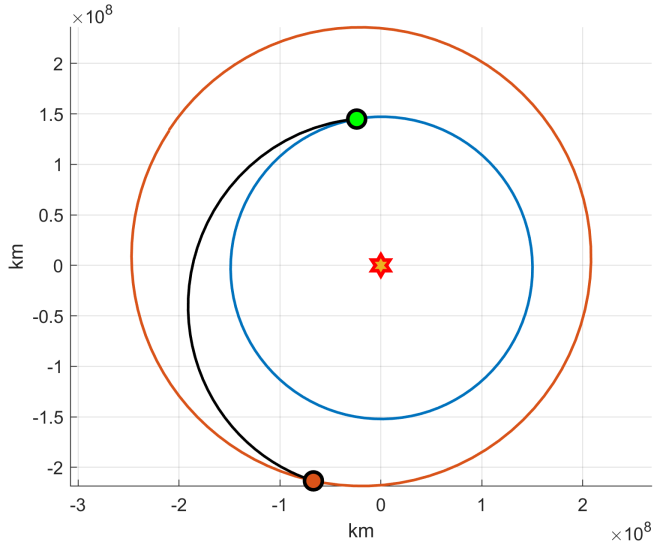


Fig. 4 Earth to Mars transfer with green marker representing Earth and Orange dot representing Mars

From solving Lambert's problem the required Δv can more accurately calculated using the parking orbit velocity and escape velocity. From further analysis done in MATLAB the Δv required to for trans mars injection was calculated to be 3.797 m/s.

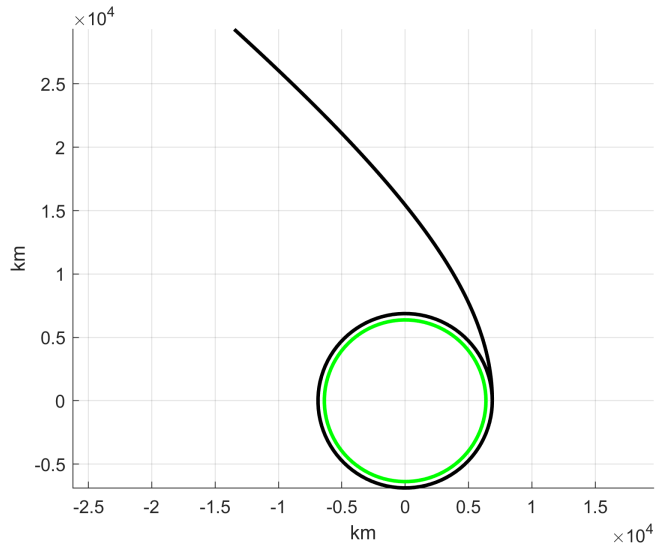


Fig. 5 Earth Departure Diagram

During transit multiple corrections are needed to keep the spacecraft on track to intersect Mars. The total duration of the coast phase from Earth to Mars is 224 Days. About 2 days before mars Periapsis the lander (AEGIS) separates from the main spacecraft. The orbiter (GALE) will perform a Mars capture burn to go into a highly eccentric orbit using 1.541 km/s of Δv . The final orbit of GALE is shown in Figure 6.

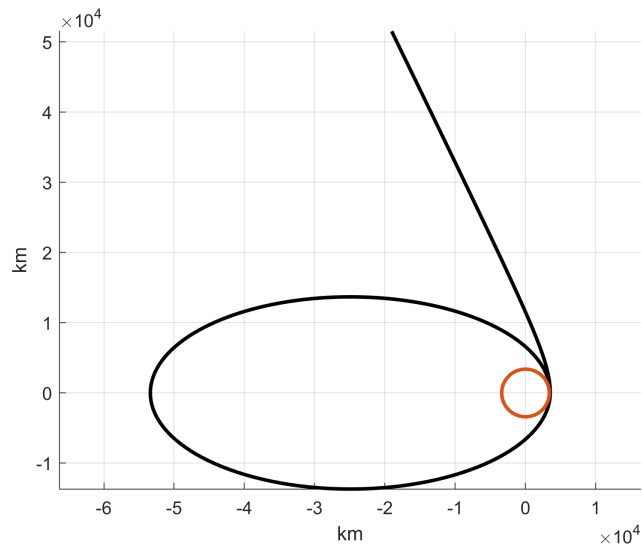


Fig. 6 Mars Arrival Diagram

3. Aerobraking Maneuvers

Once GALE is in a highly eccentric orbit the Periapsis is low enough in the Martian atmosphere where drag is non-negligible. Due to this the Apoapsis will decay over the course of months. This strategic aerobraking allows the

spacecraft to save hundreds of meters per second of Δv going from a highly eccentric orbit to one where the Apoapsis is 378 kilometers. At 378 kilometers GALE performs a burn to raise its Periapsis to get into a sun synchronous orbit. The full parameter breakdown of the orbit is shown in Table 5.

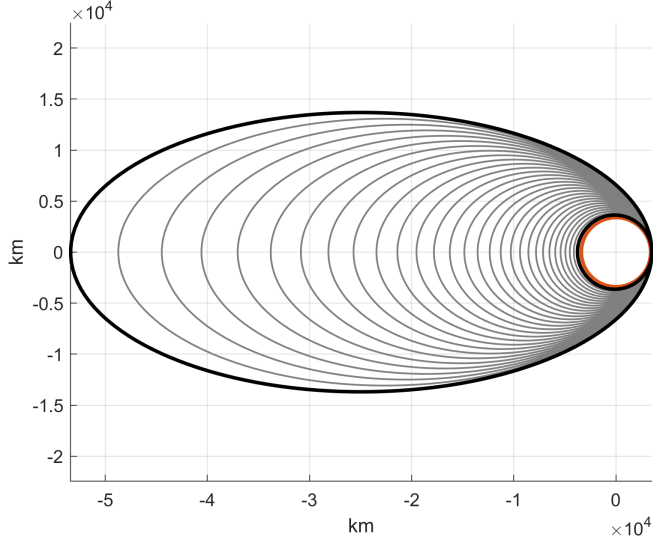


Fig. 7 Mars Aerobraking Diagram

Table 4 Table of orbital parameters for pre-aerobraking, post-aerobraking and Mars Sun Synchronous Orbit

Parameter	Pre-Aerobrake	Post-Aerobrake	Mars SSO
Semi-major Axis (km)	28450	3639	3768
Eccentricity	0.877	0.035	0
Orbital Period (s)	145693	6665	7022
Periapsis Altitude (km)	120	120	378
Apoapsis Altitude (km)	50000	378	378
Velocity at Periapsis (km/s)	4.785	3.554	3.371
Velocity at Apoapsis (km/s)	0.315	3.311	3.371

4. EDL Analysis/Simulations

Mars Entry Decent and Landing (EDL) is the riskiest part of the mission by a significant margin. Because of this a significant amount of work has been done on the EDL analysis and the interactions with other subsystems. The EDL analysis was broken into two sections: entry phase and powered decent phase. The entry phases was simulated using a 3

degree of freedom model (3DOF) and the powered decent phase was simulated using a 6 degree of freedom model (6DOF) model. The equations of motion of for the three degree of freedom model is shown below where $\rho(h)$ is the density as function of height, $g(h)$ is gravity as function of height, and R_{planet} is the radius of Mars.

$$\dot{v} = \frac{\rho(h)}{2\beta} - g(h) \cdot \sin(\gamma) \quad (1)$$

$$\dot{\gamma} = \frac{v \cdot \cos(\gamma)}{R_{\text{planet}} + h} - \frac{g(h) \cdot \cos(\gamma)}{v} \quad (2)$$

$$\dot{h} = v \cdot \sin(\gamma) \quad (3)$$

The heating was calculated using convective heat flux using equation 4 where K is Sutton–Graves constant for Mars and r_N is nose radius of the lander.

$$\dot{q} = \frac{K}{10^4} \cdot \sqrt{\frac{\rho(h)}{r_N}} \cdot v^3 \quad (4)$$

Table 5 Table of Initial conditions for 3DOF simulation

State	Variable	Initial Condition
Velocity	v	4.785 km/s
Flight path angle	γ	-13°
Height	h	135 km
Heat flux	q	0 J/s

The entry phase of flight is divided into three distinct stages. The first stage is ballistic entry, which begins at an altitude of 135 kilometers and continues down to 5 kilometers above sea level. This is where the majority of re-entry heating occurs. The second stage involves parachute deployment while the heat shield is still attached, spanning from 5 kilometers to 1 kilometer above sea level. The final stage begins at 1 kilometer and continues to approximately -6.2 kilometers, during which the heat shield separates. It is important to note that Hellas Planitia lies around 7 kilometers below Martian "sea level", placing the final descent phase well within its basin.

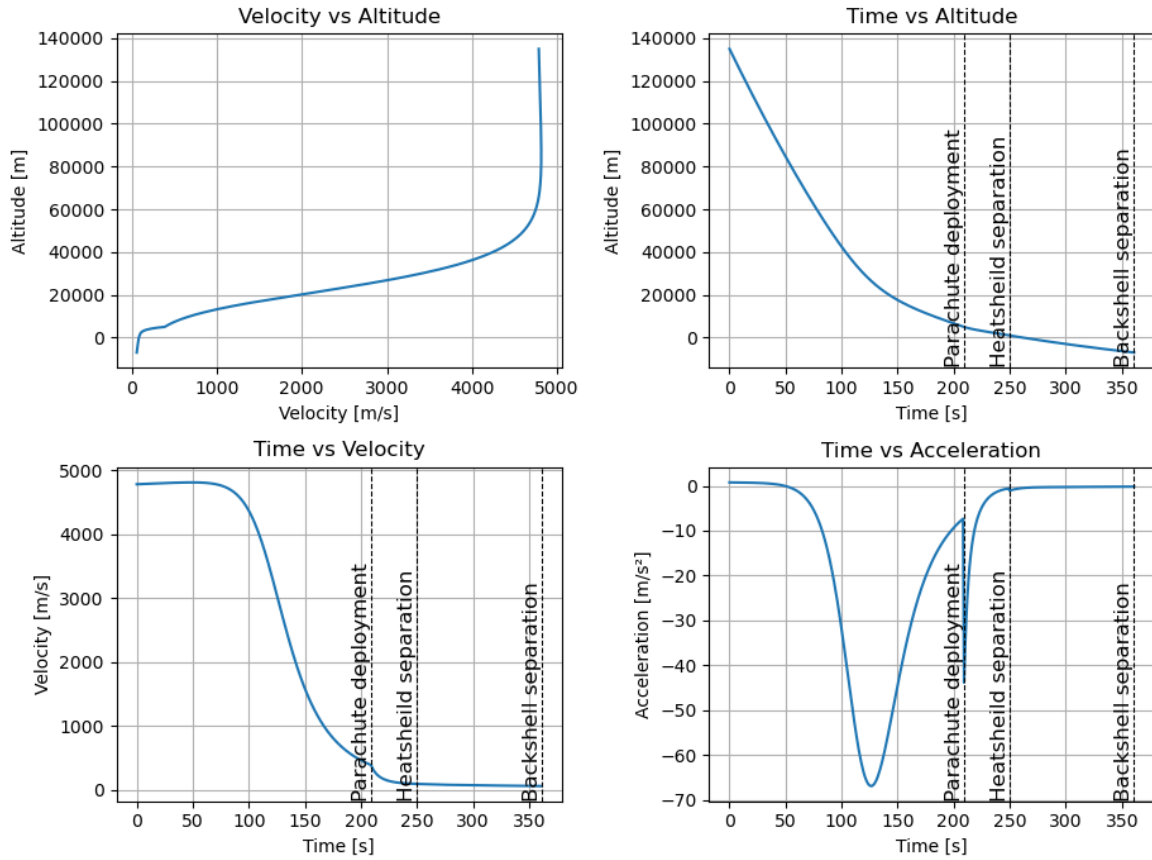


Fig. 8 Entry descent and landing profile showing velocity vs altitude (top left), time vs altitude (top right), time vs velocity (bottom left) and time vs acceleration (bottom right)

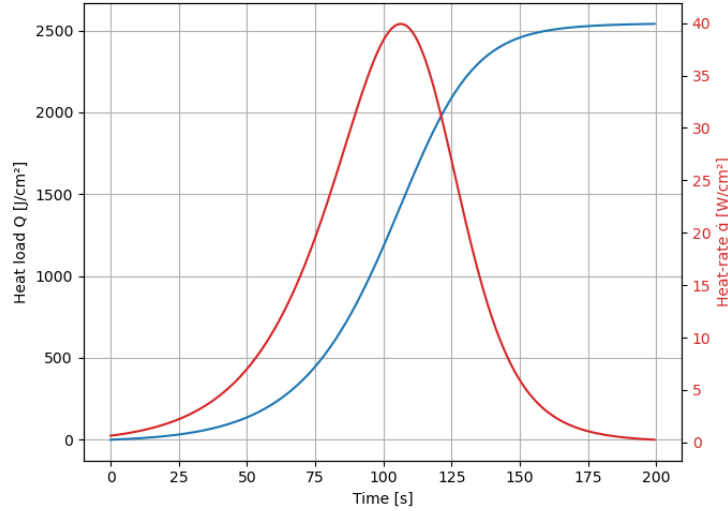


Fig. 9 Convective heating from lander showing integrated heat load and heat rate

The powered descent phase was calculated using a 6 degree of freedom trajectory optimization. The model of the

lander was assumed to be a rigid body with six thrusters with direction \hat{d}_i where i is the i^{th} thruster. Each thruster has some location \vec{l}_i from the center of mass. The main objective is to solve the minimum fuel problem given the dynamics and initial conditions. The initial condition was gathered from the final condition of the entry phase of flight and the final condition being on the surface of Mars descending at 1 m/s. The algorithm used was SCvx, a type of sequential convex programming (SCP). SCP works by reformulated the problem into a subproblem that is convex by linearizing the dynamics and constraints. The subproblem is then solved iteratively by a convex solver such as MOSEK and stops when the solution no longer changes. The non-convex formulation is shown below. [5]

$$\begin{aligned}
& \textbf{Cost Function:} \quad \min_{t_f, u} -m_f \\
& \textbf{Initial Conditions:} \quad \vec{x}(0) = \vec{x}_0 \\
& \textbf{Terminal Conditions:} \quad \vec{x}(t_f) = \vec{x}_f \\
& \textbf{Dynamics:} \quad \dot{m} = -\frac{1}{I_{sp}g_0} \sum_{i=1}^{n_u} u_i \\
& \quad \dot{\vec{r}} = \vec{v} \\
& \quad \dot{\vec{v}} = \frac{1}{m} C_l^B \sum_{i=1}^{n_u} \hat{d}_i u_i + \vec{g} \\
& \quad \dot{\vec{q}} = \frac{1}{2} \Omega(\vec{\omega}) \vec{q} \\
& \quad \dot{\vec{\omega}} = J_B^{-1} \sum_{i=1}^{n_u} \vec{l}_i \times (\hat{d}_i u_i) - \vec{\omega} \times (J_B \vec{\omega}) \\
& \textbf{Control Constraints:} \quad u_{\min} < u_i < u_{\max} \quad \forall i \in [1, n_u]
\end{aligned}$$

Due to the constant velocity section at the end of the landing optimization is technically two optimization, one for landing burn and the other is for constant velocity. Initial and final conditions of the optimization are shown in Table 6 with the parameters for the simulation shown in Table 7. The number of nodes (discretizations)

Table 6 Table of Initial and Terminal conditions for the two optimization problems

State	Initial Conditions	Start of CV	Final Condition
Position (m)	[0,0,900]	[50, 200, 8]	[50, 200, 0]
Velocity (m/s)	[0,0,-59.7]	[0,0,-1]	[0,0,-1]
Quaternion	[1,0,0,0]	[1,0,0,0]	[1,0,0,0]
Angular Rate (rad/s)	[0,0,0]	[0,0,0]	[0,0,0]

Table 7 Table of parameters for trajectory optimization

Parameter	Value
$g_0(\frac{m}{s^2})$	9.81
$I_{sp}(s)$	225
$J_b(kg \cdot m^2)$	diag(81.5, 81.5, 163)
n_u	6
$u_{min} (N)$	31
$u_{max} (N)$	1200

The results of the trajectory optimization show nominal results with only 23.5 kilograms of proponent used. The results of the optimization are shown in figure 10 and the 3D trajectory is shown in figure 11.

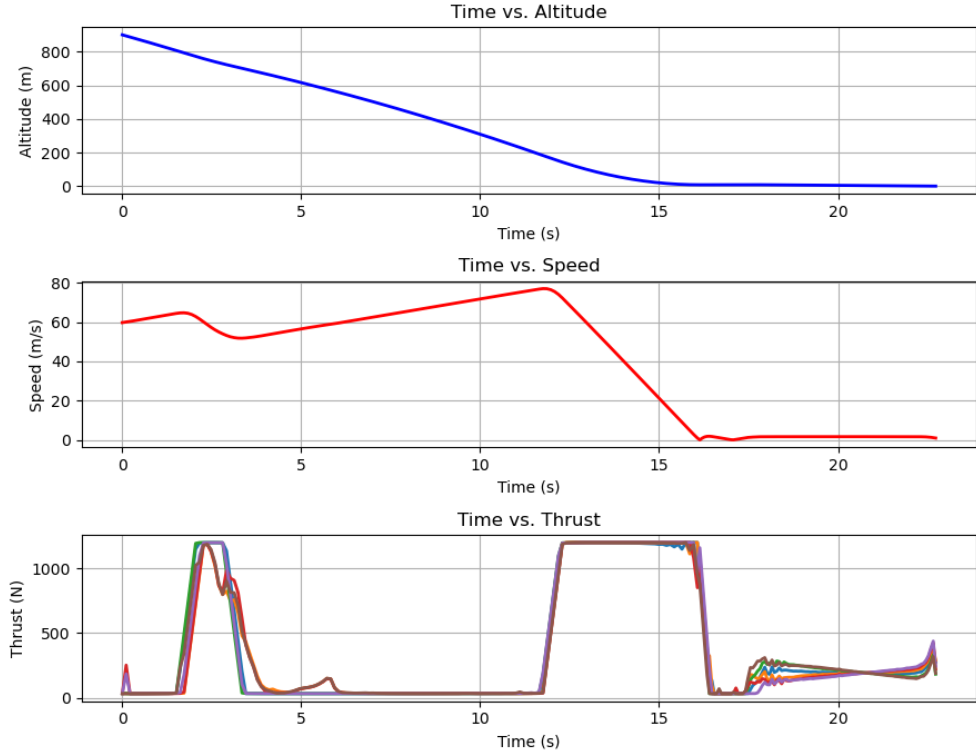


Fig. 10 Plot of Time vs. Altitude (top), Time vs Speed (middle), and Time vs Thrust for each of the 6 thrusters (bottom)

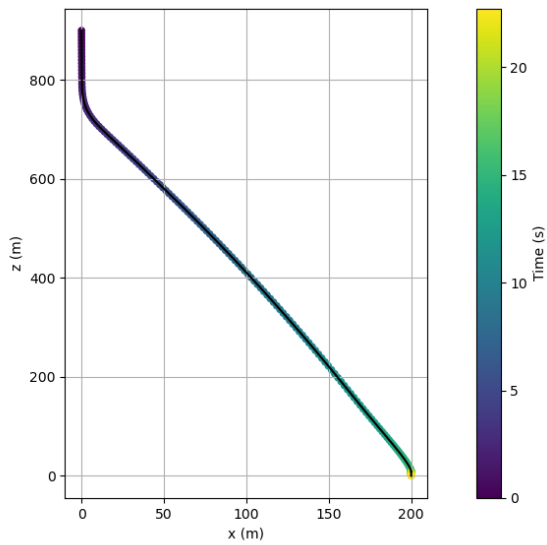


Fig. 11 2D projection of 3D trajectory for powered descent landing

B. Structures

1. Structures Requirements

These requirements found in Table ?? were chosen to ensure structural soundness throughout the mission, operational capabilities, and feasibility within budgets and vehicular capabilities.

Table 8 Top-Level Structural and Configurational Requirements

ID	Requirement	Rationale
OR-STR-01	The spacecraft shall survive the launch environment of the Falcon Heavy Launch Vehicle.	Mission should reach destination in proper form.
OR-STR-02	The spacecraft frame shall provide structural support for all subsystems and instruments during all mission phases.	All instruments and subsystems need to be fairly accommodated for their needs within the design.
OR-STR-03	The spacecraft shall enable the separation of the GALE orbiter and the AEGIS lander during Mars transfer.	The mission has components with different destinations, but will be packed together for launch.
OR-STR-04	The combined dry mass of structural subsystems, including the launch vehicle adapter, shall not exceed 1250kg.	Based on previous missions of similar architecture and/or goals.
GA-STR-01	Structures & Mechanisms shall accommodate four operational configurations corresponding to operational stages of the mission: Launch, Transit, Aero-braking, and Nominal Operations.	Each of these mission stages will have differing relative orientations to Earth & Sun, and differing key requirements necessitating configurational differences.
AE-STR-01	Lander structures shall accommodate three configurations: Stowed, Landing, and Nominal Operations.	Each of these mission stages have differing key requirements necessitating configurational differences.
AE-STR-02	Lander shall have landing legs that maintain a level platform, and support the structure.	Equipment onboard lander requires a secure platform, instruments require a steady and level platform.

2. GALE Structures

The GALE orbiter's structural design serves as the primary physical framework and support for all subsystems and instruments throughout the mission. This design is critical to withstand launch loads, operational stresses, and meeting mission requirements.

The GALE orbiter's structural design features a box-shaped configuration. This design choice aims to strike a balance between providing internal volume for accommodation of the various subsystems, ease of manufacturing, and fitting for the launch fairing. The external dimensions are as follows: 203.20cm in length and 158.75cm in width and height. These preliminary dimensions derive from comparison with analogous Mars Orbiters such as MCO, MRO, and Mars Express for starting values, then refined based on subsystem allocation and arrangement (figure 12).

The primary structure materials selected are Aluminum 6061 and CFRP (carbon-fiber reinforced polymers). Aluminum 6061 was chosen for its favorable combination of strength, cost-effectiveness, and manufacturability, while CFRP and other polymers should be used in combination to significantly reduce overall mass (Al-6061's primary

downside) at the cost of ease-of-manufacturability and expense. Alternative materials such as Aluminum 5052 and 6063, and other composites were also considered for primary structural materials, and Aluminum 7075 and Titanium alloys were also considered for stressed areas, and future design iterations should continue exploring the use of these materials for a more robust design. These material selections were inspired by considering material properties, loading conditions, and flight history on similar missions.

GALE is modeled with a thickness of 10mm, a conservative initial estimate to ensure sufficient stiffness and strength to withstand the launch loads imposed by Falcon Heavy (as stipulated by requirement OR-STR-01), and operational (structural and thermal) stresses encountered during the mission (as stipulated by requirement OR-STR-02). It's important to note that this thickness is a primary factor influencing the structural mass estimate and will be an area for further refinement after Finite Element Analysis. Initial computations were done assuming Aluminum 6061 as the primary structural material. These dimensions and material choices were driven by structural requirements to survive launch and separation, and by mass requirements, which were initially defined by adapting estimates of similar missions. An initial range of a mass estimate was 450-750kg, but with smart materials choices and structural design we have headroom, maintaining under 500kg.

All primary structural elements for GALE are designed with a minimum structural safety factor of 1.5. This factor, common in aerospace design, ensures that the structures can withstand loads significantly greater than the maximum expected operational and launch loads (OR-STR-01), providing a necessary margin against unforeseen stresses or material variability.

The current structural design is a simplified representation covering major subsystems and overall structure and organization. Future design iterations will involve further detailing, including the integration of internal stiffeners, mounting points, cutouts, and joints. Consideration of material mixes for specific components might also be explored. The overall design philosophy prioritizes cost and feasibility, aiming to utilize readily available materials and established manufacturing techniques.

3. GALE Configuration and Mechanisms

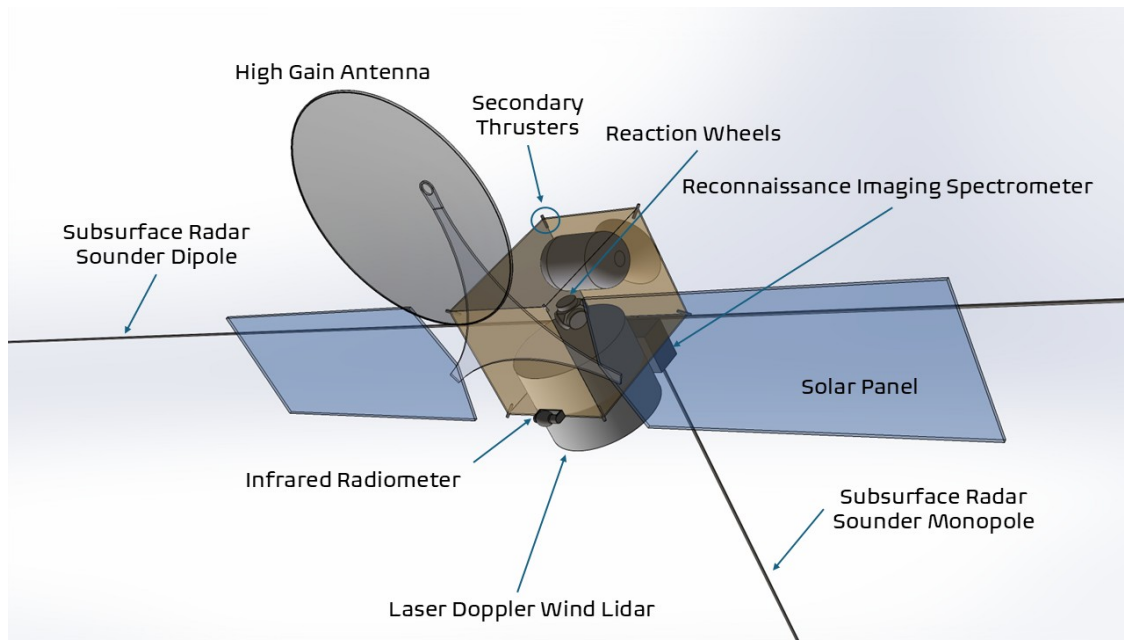


Fig. 12 System Configuration Overview

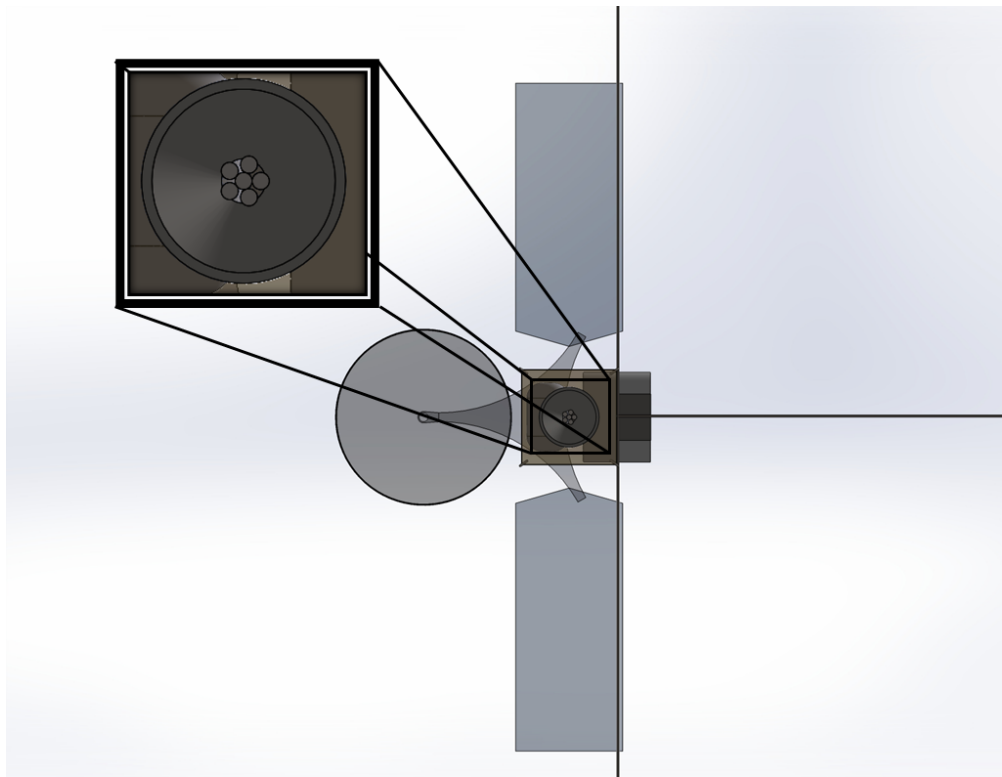


Fig. 13 System Configuration - Back View

The configuration seen in figure 12 was meticulously laid out to ensure all science payloads are properly oriented for maximal (and simultaneous) operation, while also maintaining control and navigation capabilities, and accounting for solar array and communications pointing.

Part of the key to achieving this will be the use of an **articulating solar array and high gain antenna** with wide range of articulation, in order to get more favorable pointing in otherwise sub-optimal orientations, enhancing communication and power efficiency (STR-OR-02, STR-GA-01).

While acknowledging the additional complexity that articulating mechanisms introduce to the system, the decision to include them is driven by the significant improvements they offer in both the communications link and power collection efficiency. By allotting the panels a mechanism to rotate and tilt, in order to enable optimal capture of sunlight throughout the Martian year and across different orbital orientations, GALE is ensured sufficient power generation for the mission's science objectives (GA-POW-01). Similarly, by providing the HGA a mechanism to continually adjust its pointing to maintain link with Earth, it can optimize data transmission further, and fulfill GA-COMM-02. This design decision also goes towards fulfilling the requirements outlined in STR-OR-02 and GA-OR-01.

The choice to use articulating solar arrays and a high gain antenna draws inspiration from successful missions like the Mars Reconnaissance Orbiter, which also used this approach to enhance power generation and communication capabilities, thereby supporting the mission's scientific objectives.

4. AEGIS Structure, Configuration, and Mechanisms

The AEGIS lander's structural subsystem provides the physical framework and support for all lander components, ensuring structural integrity during all mission phases, including launch, transit, entry, descent, landing, and surface operations. The design of the AEGIS lander draws inspiration from successful Mars lander missions such as InSight and Phoenix, adopting a circular base with a three-legged landing system (see figure 14). This design prioritizes stability and levelness in Hellas Planitia, considering winds, dust storms, and rough terrain.



Fig. 14 AEGIS Structural Overview

The central structural element will be a sandwich structure with primarily aluminum-based face sheets, and internal honeycomb elements. The upper "roof" platform will have a diameter of 1.5 meters, while the lower "floor" platform will have a slightly smaller diameter of 1.25 meters, consistent with Insight and Phoenix. There will be an internal volume height of 0.45m to house subsystems, with additional space on top of the "roof" platform.

AEGIS will employ a three-legged landing system, designed to provide stable support on uneven terrain. Each leg will be telescoping, and involve pneumatic actuators for post-landing leveling, as the scientific objective to ensure accurate surface measurements (related to MIS-OR-03) necessitates a level platform. This flows down to a specific structural requirement: AE-STR-02.01 and AE-STR-02.02. These legs will maintain a lander height between .835m and 1.10m, consistent with the Insight and Phoenix landers.

At this stage of design, each leg will consist of 3 Aluminum 6061 telescoping leg elements, each element consisting

of an upper leg element connecting to the main body, and a lower leg element connecting to a durable non-metal foot, where each of the three telescoping leg elements will converge. They will each be actuated via pneumatics, pressurized via a nitrogen gas tank, and utilizing aerospace grade solenoid valves for precise control, and a Tiltmeter with associated control electronics. These articulation considerations flow down from the overarching structural support requirement (OR-STR-02) and AEGIS-specific requirements (AE-STR-01).

While specific numerical values are yet to be determined, AEGIS has a levelness requirement (AE-STR-02) to ensure proper operation of surface instruments. The Levelling System will utilize a 2-axis Tiltmeter to monitor lander tilt and actuate the adjustable legs to achieve a level orientation.

The primary structural material for the AEGIS lander is 6061-T6 Aluminum Alloy. This material was chosen due to its favorable balance of strength, cost-effectiveness, and manufacturability. For high-stress areas, such as landing leg joints, the use of a Titanium alloy is being considered to provide increased strength and toughness. Additionally, 7075 aluminum is a potential candidate for critical joints or high-stress areas if further analysis indicates a need for enhanced strength. While a Carbon Fiber-Aluminum Honeycomb composite was considered for potential mass optimization, it is currently deemed overly costly for the primary structure given the project's budget constraints but may be considered for internal support in future design iterations. A preliminary trade study also evaluated other aluminum alloys 6061-T6, 6063-T6, 7050-T7451/T7651, and 7075-T6 based on key features, strength, corrosion resistance, weldability, machinability, density, relative cost, and potential applications. The study concluded to use 6061 for the main structure, with potential incorporation of titanium or composites for strength or cost considerations, and 7075 for critical joints.

While the lander does have an RTG, we will also have solar panels. These will operate similar to Insight, like seen in figure 15.



Fig. 15 Lander Deployed (Insight Shown)

Again, to note, All primary structural elements for AEGIS are designed with a minimum structural safety factor of

1.5. This factor, common in aerospace design, ensures that the structures can withstand loads significantly greater than the maximum expected operational and launch loads (OR-STR-01), providing a necessary margin against unforeseen stresses or material variability.

5. Launch Vehicle Adapter

A custom adapter is required to connect the combined spacecraft stack (GALE orbiter and AEGIS lander) to the Falcon Heavy fairing safely. The adapter will be designed to minimize the risk of separation failure, and will include a structural interface to connect to the Falcon Heavy payload attach fitting and the spacecraft stack and interfaces for any necessary instrumentation.

6. Operational Modes

This section outlines the distinct operational modes (for structural mechanisms) for the GALE orbiter and the AEGIS lander throughout the ORACLES mission.

GALE will experience four Operational Modes/Configurations:

- 1) Stowed/Launch Configuration: GALE is stowed, with solar panels folded up, and Antenna folded in, as seen in figure 16. This is in order to best pack into the fairing and protect the system.

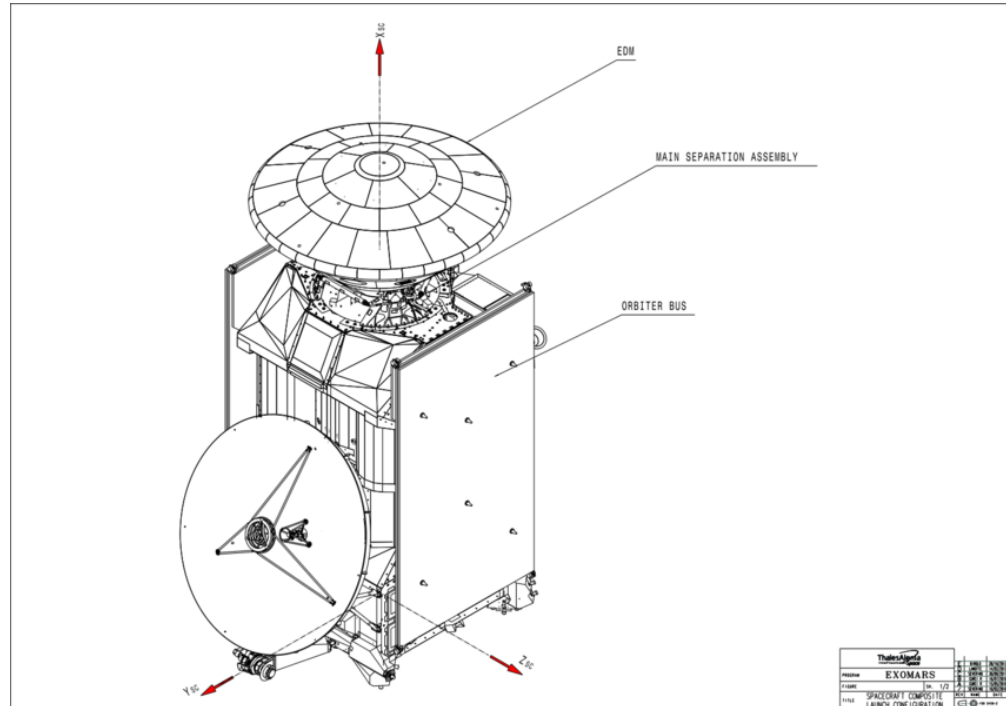


Fig. 16 Launch (Stowed) Configuration (TGO/Schiaparelli Shown)

- 2) Transit Configuration: Following separation from the launch vehicle, GALE (and AEGIS) travel to Mars over a period of multiple months. In this time, the solar panels will unfold for power generation, and Antenna will

unfold for communications. AEGIS will remain attached until the end of this mode.

- 3) Aerobraking Configuration: In this configuration, AEGIS is no longer attached, and the solar panels and Antennae remain open, but also adjust orientation to assist/account for aerobraking.

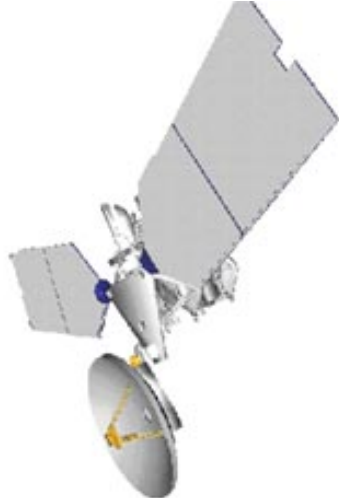


Fig. 17 Aerobraking Configuration (MRO Shown)

- 4) Nominal Operations Configuration: In this configuration, the solar panels will still track the sun, in a non-symmetric manner to maximize power collection. Additionally, the HGA will do the same for tracking earth to maximize connectivity.

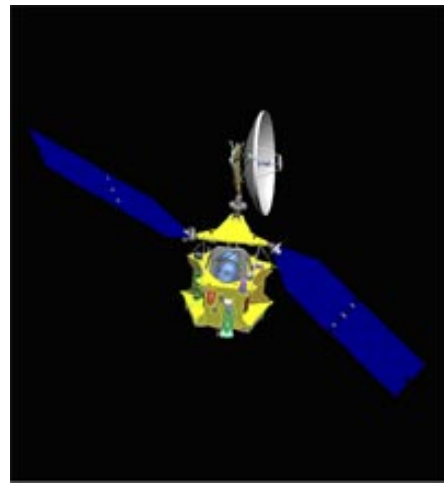


Fig. 18 Nominal Operations Configuration (MRO Shown)

AEGIS will experience three Operational Modes/Configurations:

- 1) Stowed: See figure 16. AEGIS Lander will stow on top of GALE Orbiter, legs fully retracted and solar panels fully folded in. Note, it will have an entry and descent module with which it will be encased in, unlike how Schiaparelli attempted to land. It will remain in this configuration, inside its Entry and Descent casing until the

end of atmospheric entry.

- 2) Landing: As the AEGIS lander nears the surface of Mars, it will eventually shed its Entry and Descent exterior, and the legs will outstretch before the on-board descent thrusters finally need to burn for last stages of its descent. Solar Panels will remain folded at this time.
- 3) Nominal Operations: Once Landed, landing legs will adjust for uneven terrain to level the platform. At this time, the solar panels will open up and unfurl, like seen in figure 15.

In short, The first phase of the mission will see both AEGIS and GALE stowed in the launch vehicle, then both AEGIS and GALE will deploy from the Falcon Heavy. They will operate as one "unit" until we reach AEGIS's direct injection point, at which GALE will soon also begin aerobraking and adjust its configuration as such. Similarly AEGIS will eventually near the surface and deploy. Then both systems will reach Nominal Operations configurations.

C. Electric Power System

1. EPS Requirements

Table 9 Top-Level Electric Power System Requirements

ID	Requirement	Rationale
OR-POW-01	Operational power demand shall be dictated by instrument requirements and duty cycles, and defined as the hourly average expenditure through a sol.	Average technology use should be accurately reflected in the duty cycles such that the EPS is inherently designed toward a minimum power generation.
OR-POW-02	Peak power demand shall be dictated by simultaneous instrument use and reflect increased duty cycles, relative to operational power.	Provides an additional margin to power generation and permits flexibility in operations.
OR-POW-03	End of life power generation will be scaled to reflect the 5-year mission duration.	Ensures GALE and, more necessarily, AEGIS endure the 5-year mission with minimum required power.
OR-POW-04	GALE shall supply at least 240 W during cruise to all auxiliary systems.	The RTG of AEGIS must be constantly cooled, batteries must be maintained over respective discharge levels, and the health of the architecture must be continuously monitored.
OR-POW-05	The Entry, Descent and Landing module shall use a primary battery supply, separated from the GALE or AEGIS power solutions.	The power demand profile for the module is very distinct from either vehicle and only needs to supply power through atmospheric descent.

2. GALE

The Electric Power System (EPS) onboard the GALE Orbiter is designed to continuously generate sufficient power for operational power cycling, and rely an ancillary supply to meet peak power demands. The operational power budget and peak power cycle budget are outlined in Tables 10 and 11, respectively. A growth allowance of 20% is attached to each subsystem item. The duty cycles were determined according to mission priority, operation requirements, or

thermal requirements.

To generate operational power, the EPS benefits from the sun-synchronous orbit of GALE, drawing 1506.2 W in solar power throughout the entirety of the orbit. An additional growth factor was added to account for simultaneous instrumentation operation, hence the discrepancy between operational power generated and demand. While various fluctuations in solar irradiance may be present, whether through eclipses or standard orbital variation, solar irradiance was calculated assuming a constant average flux of 585.99. Excess gained via the 20% growth allowance and standard fluctuations will be stored in secondary batteries, meant to handle peak power loading.

Solar panel calculations were determined according to a five year mission duration and used industry standard efficiency values: inherent degradation of 2.75%, solar array efficiency of 85%, temperature efficiency of 85%, maximum zenith angle deviation of 6.5°. Multi-junction gallium arsenide (GaAs) solar cells were selected due to their high cell efficiency of 22.6%. To meet the operational power demand, 18.56 m² of GaAs (MJ) solar cells are required. Two rechargeable lithium-ion (Li-Ion) batteries are used to meet peak power demand. Given that the spacecraft bus voltage is 28 V, determined according to the scale of power demands, the battery system requires 35.50 Ah. With redundancy, this falls to 11.83 Ah, but we introduce an additional growth allowance to accommodate an industry standard of 15 Ah. This is summarized in Table 15.

Table 10 Operational Power Budget for GALE

Subsystem ID	Subsystem Item	Estimated Power per Unit (W)	QTY	Predicted Power per Unit (W)	Duty Cycle (%)	Total Power (W)
INSTR	Laser Doppler Wind Lidar	840	1	1008	25%	252
	Reconnaissance Imaging Spectrometer	47.3	1	56.8	75%	42.6
	Infrared Radiometer	11	1	13.2	7%	0.88
	Subsurface Radar Sounder	60	1	72	50%	36
COMM	Flight Computer	11.5	2	13.8	100%	13.8
	Band UHF Transmitter	10	1	12	1%	0.1332
	Band Xband Transmitter	100	2	120	33%	79.2
TCS	HVAC	424	1	508.8	100%	508.8
ACS	Reaction Wheel	40	4	48	50%	96
	IMU	30	1	36	100%	36
PROP	Main Propulsion Thruster	83	6	99.6	10%	0
	RCS Thruster	36	8	43.2	5%	17.28
Total						1156.2

Table 11 Peak Power Budget for GALE

Subsystem ID	Subsystem Item	Estimated Power per Unit (W)	QTY	Predicted Power per Unit (W)	Duty Cycle (%)	Total Power (W)
INSTR	Laser Doppler Wind Lidar	840	1	1008	100%	1008
	Reconnaissance Imaging Spectrometer	47.3	1	56.8	100%	56.8
	Infrared Radiometer	11	1	13.2	7%	0.88
	Subsurface Radar Sounder	60	1	72	100%	72
COMM	Flight Computer	11.5	2	13.8	100%	27.6
	Band UHF Transmitter	10	1	12	1%	0.1332
	Band Xband Transmitter	100	2	120	33%	79.2
TCS	HVAC	424	1	508.8	100%	508.8
ACS	Reaction Wheel	40	4	48	50%	96
	IMU	30	1	36	100%	36
PROP	Main Propulsion Thruster	83	6	99.6	100%	597.6
	RCS Thruster	36	8	43.2	5%	17.28
Total						2500.3

3. Entry, Descent, and Landing

The Entry, Descent, and Landing (EDL) EPS architecture necessitates that it be isolated from the power solutions developed for GALE and AEGIS. Because EDL occurs in roughly 6.5 minutes, the power draw and demand of EDL will either require very high power load or a high current load, dependent on if the demand is continuous or instantaneous. These systems are characterized in Table 12. High power items are continuously powered through EDL as necessary per mission and trajectory requirements. High current items are related to instantaneous events through EDL that have upwards of 45 A drawn for a pyrotechnic actuation or mortar firing. The power demand of these items are drawn directly from reference values, when possible.

Table 12 Power Consumption through Entry, Descent and Landing

Characterization	Subsystem Item	Estimated Power (W)	Operation Duration
Continuous	Aero thermal Sensor Suite	30	100%
	Descent Camera	3	100%
	Radar Doppler Altimeter	70	33%
	Landing Thruster (6x)	144	20%
	RCS Thruster (8x)	288	20%
Instantaneous	Parachute Deployment	-	-
	Heatshield Jettison	-	-
	Backshell Jettison	-	-

Per the highest potential power consumption, the continuous system is sized for a 288 W power supply, resulting in a

102 Ah Lithium-Ion power supply per the 28 V supplied by the unregulated EDL EPS architecture. The instantaneous events lacked the literature to make appropriate quantitative estimates. Instead, similar mission profiles were investigated to determine the available power supply rather than specific required amount. Based on the ExoMars 2016 mission, the instantaneous power demand will be met by a high rate 3.3 Ah power supply.

4. AEGIS Lander

Hellas Planitia poses a significant challenge for the EPS of the AEGIS lander. As a site of frequent dust storms, solar panels can be unreliable, which typically lends to the use of fuel cells or primary batteries. However, these result in a very short mission life, on the order of a few hours to a few days at most. ORACLES is interested in investigating and monitoring the Hellas Planitia landing site for the mission duration to better understand dust storm formation and activity on Mars. To accommodate the mission duration, an alternative power solution is necessary.

The EPS of AEGIS is derived from the lander's various power cycles per ???. The operational power cycle is defined in Table 14. Duty cycles for instrumentation were designed according to individual requirements and maintenance needs. The devised system splits a Martian hour between the saltation sensor, microARES electric field sensor, laser doppler dust anemometer, and ambient environment sensors. The imagining camera takes a series of pictures at the start of each hour. This occurs for a cumulative 23 Martian hours. The final hour is split between transmitting data to the orbiter and maintaining the power solution. This results in a more specific set of power demands according to each cycle. The actual operational power budget, accommodating scientific instrumentation, thermal control, and the flight computer, requires 114.09 W. The peak power budget, dictated by transmission and maintenance, requires 167.13 W. Idling power sits at 98.46 W, where only the flight computer and thermal control system are in operation.

Table 13 AEGIS Power Modes

Mode	Operating Systems	Power Draw (W)
Idle	TCS + FC(IDLE)	98.46
Operations	TCS + FC(DH) + INSTR	114.09
Peak Cycling	TCS + FC(DH) + COMM + SOLAR	123.8 + 43.33

Table 14 Operational Power Budget for AEGIS

Subsystem ID	Subsystem Item	Estimated		Predicted		Duty	Total
		Power per Unit (W)	QTY	Power per Unit (W)	Cycle (%)	(W)	
INSTR	Saltation Sensor	0.03	1	0.036	25%	0.009	
	Radiation Assessment Detector	4.2	1	5.04	25%	1.26	
	Imaging Camera	11.8	1	14.16	2.5%	0.354	
	Thermo(pile/couple)	0.604	3	0.724	8.3%	0.1811	
	Pressure Transducer	1.811	1	2.173	8.3%	0.1811	
	2D Wind Sensor	1.811	1	2.173	8.3%	0.1811	
	MicroARES Electric Field Sensor	0.85	1	1.02	2.5%	0.0255	
	Solar Irradiance Sensor	0.4	1	0.48	12.5%	0.06	
	Laser Doppler Dust Anemometer	0.14	1	0.168	25%	0.042	
COMM	Flight Computer	11.5	1	13.8	100%	13.8	
	UHF Transmitter	10	1	12	2%	0.24	
TCS	HVAC	98	1	117.6	83%	97.608	
Total							113.9

The multi-mission radioisotope thermoelectric generator (MMRTG) was selected for ORACLES. Standard production and deployment fall within budget, but the required research and development necessary to accommodate the power demand of AEGIS would be too expensive. Instead, the MMRTG is accompanied by GaAs (MJ) solar panels and a singular Li-Ion battery. The solar panels are sized according to the worst-case solar irradiance conditions, determined by the Mars Climate Database. These conditions were iteratively determined based on available data and are shown in Figure 19. Because dust storms only occur for half the year, an equivalent contour plot could not be made for dusty conditions. Instead, the lowest flux dates in nominal conditions were selected, and dusty conditions were superimposed to determine the lowest potential flux. In this worst case, assuming clean panels, 383.04 Wh are available to AEGIS throughout a sol. This separates the average and best-case by an order of magnitude. To ensure effective operation, solar panels will be routinely cleaned by a high voltage electric discharge, costing 10 W per m². Should dust activity excessively limit power generation, AEGIS can idle until conditions clear, while still being capable of operating

instrumentation a few times a day, with transmission occurring every few days. The power solution of AEGIS is summarized in Table 15.

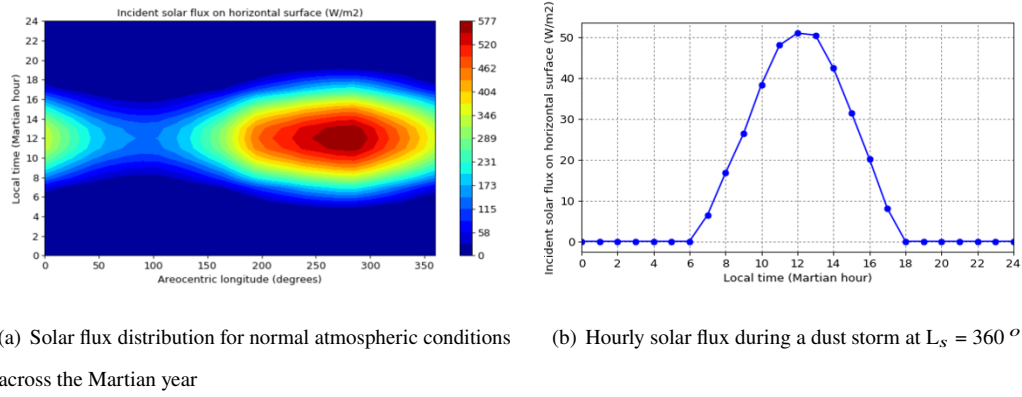


Fig. 19 Incident Solar Flux in Hellas Planitia 42.4° S, 70.5° E)

Table 15 GALE and AEGIS Power Solution

Source	GALE		AEGIS	
	Specification	Output (W)	Specification	Output (W)
Solar	GaAs (MJ), 18.56 m^2	1506.2	GaAs (MJ), 4.33 m^2	4.202
Battery	Li-Ion, 3x 8s10p	1260	Li-Ion, 8s3p	57.70
RTG	-	-	MMRTG	110

D. Propulsion System

The propulsion systems on GALE and AEGIS serve to maneuver each vehicle into the various orbits required for each vehicle at different stages of the mission. Both vehicles will have two separate systems - GALE's main propulsion system for orbital maneuvers and its attitude control propulsion system for momentum dumping, and AEGIS's main propulsion system for the soft landing and its attitude control propulsion system for stability during Mars entry. The primary requirements for these propulsion systems are shown below in Table 16, while the full list of subsystem requirements can be found in Appendix A, Table 44.

1. Propulsion Requirements

Table 16 Top-Level Propulsion System Requirements

ID	Requirement	Rationale
GA-PROP-01	The main propulsion unit shall produce at least 2.5 km/s of Δv .	Ensures the spacecraft has enough Δv to capture at Mars and maintain its orbit throughout the mission.
GA-PROP-05	The RCS propulsion unit shall produce at least 300,000 N-s of impulse.	Ensures the spacecraft can desaturate its reaction wheels frequently.
AE-PROP-01	The main propulsion unit shall produce at least 500 m/s of Δv .	Ensures the spacecraft has enough Δv to safely land on the Martian surface.
AE-PROP-06	The RCS propulsion unit shall produce at least 5000 N-s of impulse.	Ensures the spacecraft can maintain stability for the duration of entry.

2. GALE

GALE's primary propulsion system will be responsible for three aspects of the mission: the midcourse correction burn on the way to Mars, the capture burn to prepare for aerobraking, and station keeping maneuvers for the remainder of the mission. Based on trajectory simulations, the estimated combined Δv required for these parts of the mission is 2.5 km/s. To reasonably accommodate this large Δv requirement, a high-efficiency, high-throughput thruster is a necessity. TRL and system complexity were also considered, which limited the propellant type to a monopropellant system. Ideally, AF-M315E propellant could be used for its high density impulse, nonexistent freezing point, and ease to work with compared to hydrazine, but its low TRL (as shown in Figure 17) would necessitate significant redundancies and timeline delays that would exceed the allocated mission budget and timeline. Accordingly, hydrazine was chosen as the monopropellant fuel, and the list of potential thrusters shown in Table 18 all have the aforementioned required characteristics, with the added benefit of currently being in production by their respective manufacturers. From this selection, Moog's MONARC-90 Thruster (pictured in Figure 20(a)) suited these requirements best with the highest specific impulse of the selection, sufficient thrust, and an excess of potential total impulse. While four of these thrusters could easily suit the mission's needs, the decision was made to use six thrusters instead, allowing up to two thrusters to fail before capture at Mars, and up to four thrusters to fail after capture.

Table 17 Properties of Monopropellant Fuels for Propulsion Systems

Propellant	Density Impulse	Freezing Point	Boiling Point	TRL	Other Notes
Hydrazine	225–245 N·s/m ³	2°C	113.5°C	9	Requires SCAPE suit and SCBA to handle safely
AF-M315E	350–380 N·s/m ³	Glasses at -80°C	Autoignition at 140°C	3	Can be handled safely with nitrile gloves

For GALE’s RCS thrusters, the main requirements were high efficiency, low thrust, and low minimum impulse bit to provide maximum accuracy for momentum dumping. The Aerojet Rocketdyne MR-106L thruster (pictured in Figure 20(b)) satisfies all of these requirements, with the highest specific impulse in the low-thrust range and a minimum impulse bit of 0.015 N·sec over a 16 millisecond pulse. As GALE’s momentum wheels saturate throughout the lifetime of the vehicle, the eight RCS thrusters will occasionally fire to cancel out the angular momentum stored in the reaction wheels, allowing them to capture additional angular momentum in the future.

3. AEGIS

AEGIS’s primary propulsion will be responsible for the vehicle’s final trajectory corrections before its Mars encounter and landing the vehicle softly on the Martian surface as the last phase of EDL. For the soft landing, AEGIS requires roughly 15 m/s^2 of acceleration or about 14kN of thrust. Although most manufacturers only produce hydrazine thrusters rated for less than 1kN, Aerojet Rocketdyne’s MR-80B hydrazine thruster (shown in Figure 20(c)) produces 3.1kN of thrust in nominal operation and up to 3.6kN at peak performance. As such, six of these thrusters were chosen for redundancy, though the MR-80B’s role in the Perseverance mission’s sky crane maneuver demonstrates the reliability of this model [6]. Nevertheless, having six thrusters means that the lander has two redundant pairs, since it could theoretically land with just a single pair of opposing thrusters in an emergency.

Although AEGIS won’t be spending as much time in space as GALE, it still needs an RCS system to survive Mars entry. From the time of separation, the lander will have to maintain its attitude for course corrections and communication, making it essential that the reaction wheels don’t completely saturate. With eight MR-106L thrusters aboard, the lander will be able to easily orient itself from the time it separates from GALE to touchdown. The RCS thrusters will also be active during Mars entry, providing additional stability for the vehicle as it decelerates through the tenuous atmosphere.

Table 18 Properties of Hydrazine Monopropellant Thrusters

Thruster	Manufacturer	Thrust (N)	Specific Impulse (s)	Total Impulse (kN-s)	Mass (kg)
MR-106L	Aerojet Rocketdyne	22	231	561.4	0.59
MR-107T	Aerojet Rocketdyne	110	223	162.4	1.01
MR-107S	Aerojet Rocketdyne	275	230	337.6	1.01
MR-107U	Aerojet Rocketdyne	300	226	102.7	1.38
MR-107V	Aerojet Rocketdyne	300	226	362.3	1.01
MR-80B	Aerojet Rocketdyne	3100	225	2196.2	8.51
MONARC-22-6	Moog, Inc.	22	229	533.8	0.72
MONARC-22-12	Moog, Inc.	22	228	1173.1	0.69
MONARC-90LT	Moog, Inc.	90	232	3500	1.12
MONARC-90HT	Moog, Inc.	116	234	2042.2	1.12

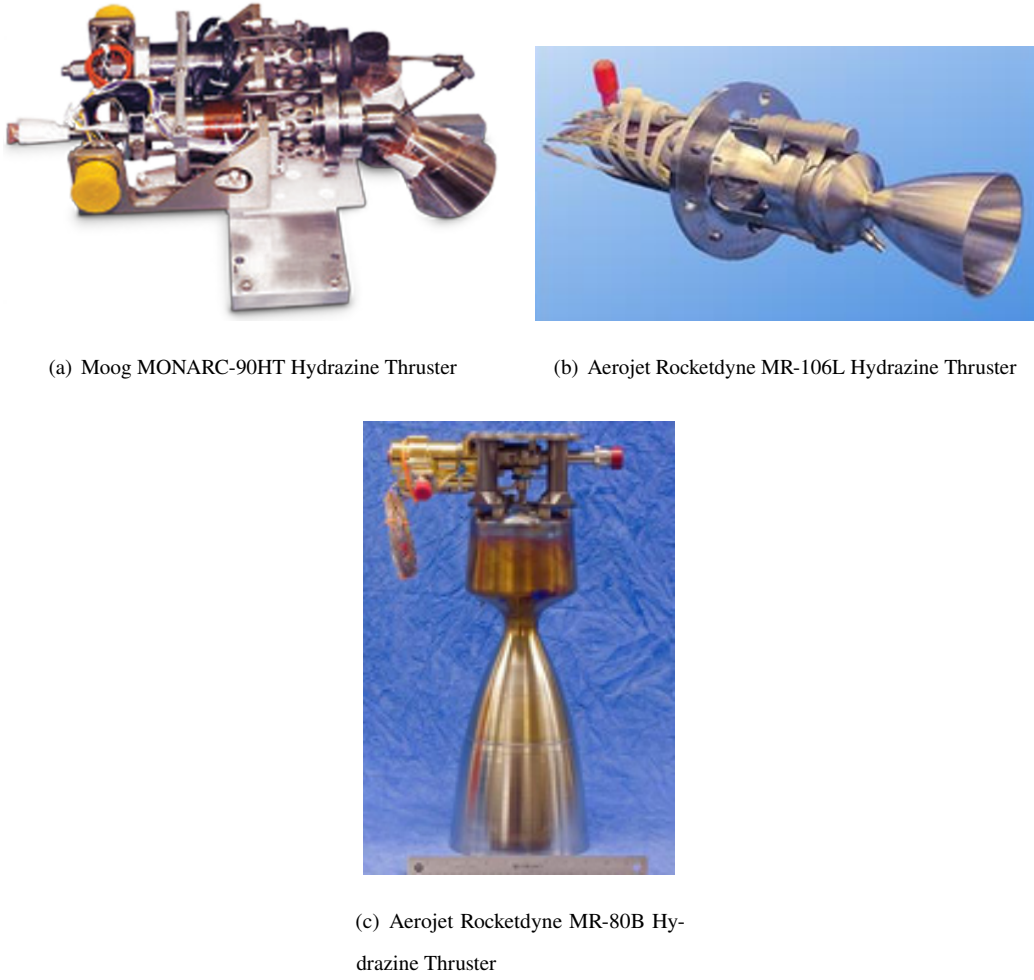


Fig. 20 Thrusters used on GALE and AEGIS.

E. Thermal Control System

1. TCS Requirements

The thermal control system (TCS) is responsible for the thermal balance of GALE and AEGIS by utilizing both active and passive methods for temperature range maintenance. This is done to ensure all mission and science requirements are fulfilled. The main requirements for the TCS are presented in Table 19; for the full list of subsystem requirements reference Appendix A.

Table 19 Top-Level Thermal Control System Requirements

ID	Requirement	Rationale
OR-TCS-01	Each body shall be equipped with a thermal control system capable of maintaining all structural and within their specified operational temperature ranges under all mission phases.	Ensures survivability and performance of core spacecraft systems during all mission phases
OR-TCS-02	Each scientific instrument shall be provided with an integrated thermal control system that maintains the instrument within its required operational temperature range throughout its mission timeline.	Preserves instrument functionality and protects sensitive hardware from thermal degradation
OR-TCS-03	Each thermal control subsystem shall include at least one redundant thermal management method.	Increases system robustness in the event of failure or unexpected thermal loading
AE-TCS-01	The lander's thermal protection system shall be designed to ensure thermal survivability during all phases of Entry, Descent, and Landing in accordance with predicted heating profiles.	Ensures lander integrity and instrument survival during EDL through proper thermal shielding

2. *EDL*

The thermal control for Entry, Descent, and Landing (EDL) consists mainly of the design of the heat shield. This design can be broken down into chosen metrics based on previous missions and calculated metrics using known equations. Quantities such as peak heat flux, air density at peak heating, as well as shield thickness and mass, can be calculated, while the heat shield material and nose radius are selected parameters.

The designed heat shield material was chosen based on the NASA Mars InSight mission, with the material being SLA-561V (Super Lightweight Ablator 561V). This material was developed by Lockheed Martin and is a proven space-grade choice to use for the heat shield in the ORACLES mission. The other chosen metric is the nose radius. This value was selected to fit the geometry and overall sizing of the lander itself, as well as to align with other similar mission choices, and has been set to be three meters.

The first solved metric is the air density at the height of peak heat. Based on the simulations and design of the trajectory for the mission, this height is determined to be $h = 100,000$ m. With a scale height $H = 10,600$ m and surface atmospheric density $\rho_0 = 0.020 \text{ kg/m}^3$, the air density ρ at the desired height can be found using the following equation:

$$\rho = \rho_0 \cdot e^{-h/H} \quad (5)$$

$$\rho = 1.5992 \times 10^{-6} \text{ kg/m}^3$$

With this air density known, the peak convective heat flux can then be calculated using the Sutton-Graves equation

shown below, where k_{Mars} is the Sutton-Graves constant for Mars, R_N is the nose radius, and V is the entry velocity determined through trajectory design:

$$q_{\text{conv}} = k_{\text{Mars}} \cdot \sqrt{\frac{\rho}{R_N}} \cdot V^3 \quad (6)$$

$$q_{\text{conv}} = 1.5172 \times 10^4 \text{ W/m}^2$$

The required thickness for the heat shield based on this heat flux is then found using the equation below, where k_{TPS} is the thermal conductivity of SLA-561V, T_s is the maximum surface temperature, and T_i is the allowable internal temperature:

$$t_{\text{TPS}} = 100 \cdot \frac{k_{\text{TPS}}(T_s - T_i)}{q_{\text{conv}}} \quad (7)$$

$$t_{\text{TPS}} = 0.2689 \text{ cm}$$

Next, the surface area of the heat shield can be determined using the lander mass m , an allowable acceleration $a = 5g$, a drag coefficient $C_D = 1.3$, and the dynamic pressure equation:

$$F = m \cdot a = \frac{1}{2} \cdot \rho \cdot V^2 \cdot C_D \cdot A \quad (8)$$

Solving for A , the area is found to be:

$$A = 674.03 \text{ m}^2$$

Finally, the mass of the heat shield can be found using the chosen material's density ρ_{TPS} , and the previously calculated area and thickness:

$$m_{\text{TPS}} = \rho_{\text{TPS}} \cdot A \cdot t_{\text{TPS}} \quad (9)$$

$$m_{\text{TPS}} = 489.39 \text{ kg}$$

3. GALE

Thermal control for the GALE orbiter includes insulation and heat dissipation for both the main body, and the instruments. The systems created for this control have been broken down and created based on the specific needs and acceptable temperature ranges of each area. For the main body, multi-layer insulation (or MLI) will encompass the inner area. This will be done with twenty coatings, adding a total of 9.84 kg of insulation.

The GALE orbiter has four instruments in need of consideration for thermal control. These instruments are the Laser Doppler Wind Lidar, the Reconnaissance Imaging Spectrometer, the Infrared Radiometer, and the Subsurface Radar Sounder. The operating temperature ranges for these instruments are seen in Table 20.

In order to keep these instruments within these ranges or at their specified temperatures, precise thermal control must be implemented. In addition to this, the control must have redundancies to ensure the temperature is never outside

Table 20 Instrument Temperature Ranges

Instrument	Temperature Range (°C)
Laser Doppler Wind Lidar	-30
Reconnaissance Imaging Spectrometer	-148.15
Infrared Radiometer	-5 to 50
Subsurface Radar Sounder	-150 to 250

of the required range. To keep the required precision, both passive and active thermal control strategies will need to be implemented. The chosen passive strategies are multi-layer insulation (MLI) and loop heat pipes (LHPs). The active strategies are cryocoolers, kapton heaters, and variable emissivity radiators. The purpose of each of these strategies are shown in Table 21.

Table 21 Thermal Hardware and Their Applications

Thermal Hardware	Purpose
MLI	Reduces heat loss
Loop Heat Pipes	Transfers heat to radiators
Variable Emissivity Radiators	Adjusts heat rejection
Cryocooler	Cooling to -148.15°C
Kapton Film Heaters	Provides emergency heating

Additionally, a breakdown of what solution is used for each instrument is also seen in Table 22.

Table 22 Thermal Solutions for Space Instruments

Instrument	Thermal Hardware
Reconnaissance Imaging Spectrometer	Cryocooler, Radiator, LHP, MLI
Wind Lidar, Infrared Radiometer, Subsurface Radar Sounder	Cryocooler, Radiator, LHP, MLI
Reaction Wheels	Kapton heaters

The selected hardware must be space-grade, capable of withstanding environmental conditions during mission operation, and designed with power consumption, mass, and cost in mind. A key advantage of the MLI thermal system is its light weight, low emissivity, and success in MRO and MAVEN. NASA has also endorsed LHPs for their ability to provide passive heat transport, while the radiators can adjust heat rejection and reduce the overall power demand of the thermal control system. Northrop Grumman's cryocooler is efficient, space-proven, and capable of maintaining the instruments at their cooler required temperatures. Finally, the Kapton heaters are both lightweight and flexible, making them a cost-effective solution for maintaining heat on the reaction wheels. The specifics and mass contributions of these components are detailed in Table 27 while the power requirements for the orbiter thermal control are outlined in Table 28. These power requirements were based on 100 percent duty cycles in order to ensure instruments were always kept in

operating and survival temperature ranges.

Table 23 Inventory and Total Mass of Thermal Components

Item	Manufacturer	Quantity	Total Mass
Instrument MLI	Admatis	8	2.20
Loop Heat Pipes	Arquimea	4	2.20
Radiators	HiPer	2	2.64
Cryocoolers	Northrop Grumman	2	9.90
Main Body MLI	Admatis	20	216.48
Kapton Heaters	Minco	12	1.32

Table 24 Orbiter Thermal Hardware Power Requirements

Thermal Hardware	Nominal Power per Unit (W)	Quantity	Power (W)
Kapton Heaters	5	12	60
Variable Emissivity Radiators	2	2	4
Cryocoolers	180	2	360

Based on these totals, the mass added will be approximately 234.74 kg, while the power needed will be about 424 W. Several trade studies were conducted to evaluate thermal control strategies for the orbiter's instruments, with an emphasis on minimizing power draw while maintaining sufficient thermal protection. The first trade study done for choosing between an active or passive radiator. A passive radiator would allow for heat dissipation without any power usage, but would be less controlled. The chosen variable emissivity radiators allow for precision and are adaptable for the occurrence of excitations to the thermal profile of the system. Another trade study was done to choose between an active Kapton film heater or passive radioisotope heating units. The decision was based on an overall assessment of the heaters' roles and the power budget, as the additional power requirements were not significant enough to outweigh the advantages of the active method in terms of mass, stability, and efficiency. Another trade study was conducted to choose between a multitude of cryocooler options. Although there were options with lower power draw or greater cooling power, the Northrop Grumman HEC provided the best balance of the two, with 180 W of nominal power and 23W cooling at 150 K.

4. AEGIS

AEGIS has eleven instruments to consider for thermal protection outside of EDL, and their operating temperature ranges can be seen in Table 25. Also in this table are designated group numbers. In order to simplify thermal control for the lander, grouping of instruments with similar temperature ranges was done to allow for less overall thermal hardware. The three groups make up instruments with colder ranges, moderate ranges, and a higher range. The temperature ranges for these groups are -130°C to 50°C for group 1, -20°C to 40°C, and 5°C to 35° for group 3. With such large ranges,

precision of temperature can be lower than for the instruments on the orbiter. This is necessary, as the climate and conditions on Mars, and specifically inside Hellas Planitia, will inherently be less predictable than those in orbit.

Table 25 Instrument Groups and Operating Temperature Ranges

Group	Instrument	Operating Temperature Range (°C)
1	Saltation Sensor	-115 to 204
	Thermometers	-130 to 70
	Barometers	-130 to 70
	2D Wind Sensor	-130 to 70
	MicroARES Electric Field Sensor	-204 to 50
	Solar Irradiance Sensor / Flux Radiometer	-130 to 70
2	Radar Doppler Altimeter	-150 to 250
	Radiation Assessment Detector	-20 to 55
	Imaging Cameras	-40 to 40
3	Descent Camera	-55 to 50
	Laser Doppler Dust Velocimeter / Anemometer	5 to 35

The thermal control strategies for these groups are very similar to that of the orbiter, just on a smaller scale. Each group has the same hardware pairings for consistency and simplicity. Table 26 outlines these thermal strategies.

Table 26 Thermal Hardware Usage and Purpose

Thermal Hardware	Purpose
MLI	Reduce heat loss
Loop Heat Pipes	Passively circulate
Variable Emissivity Radiators	Adjust heat rejection
Thermoelectric Coolers	High delta cooling
Mechanically Pumped Fluid Loops	Actively circulate

The hardware listed above serves the same overall functions as on the orbiter. MLI reduces radiative heat loss and stabilizes temperature fluctuations, while heaters provide active heating in cold conditions. TECs allow for large changes in temperature, and LHPs transfer excess heat from instruments to radiators. MPFLs manage heat dissipation, and radiators passively release excess heat when temperatures rise too high. The actual hardware chosen for the lander are almost all the same products chosen for the orbiter. These were chosen on similar bases, including the lightweight spaceproven insulation for MLI, the ability to provide direct heat to sensitive instruments for the micro heaters, the precise active cooling for the TECs, the passive heat transport for the LHPs, the ability to add redundancy in an efficient way for the MPFL, and the dynamic abilities for the radiators.

One main trade study needed for the thermal control system of AEGIS was the solution for the 1800 W of heat exhaustion coming from the RTG. The method chosen utilized the transfer of this heat through the loops into the

Table 27 Inventory and Total Mass of Thermal Components

Item	Manufacturer	Quantity	Total Mass
Instrument MLI	Admatis	12	3.30
Loop Heat Pipes	Arquimea	3	1.65
Radiators	HiPer	3	3.96
Thermoelectric Coolers	Melcor	3	0.66
Mechanically Pumped Fluid Loops	JPL	3	6.6

Table 28 Orbiter Thermal Hardware Power Requirements

Thermal Hardware	Nominal Power per Unit (W)	Quantity	Power (W)
Thermoelectric Coolers	0.67	3	3
Variable Emissivity Radiators	2	3	6
Mechanically Pumped Fluid Loops	30	3	90

radiators. After this, common estimates show about ten percent, or 180 W of heat, would still need to be transferred, and this was used for the choice of the TEC.

With the operating temperature ranges known, the change in temperature from the cold side of the radiator to the instrument groupings could be found and used in the selection of what ΔT was needed for the TEC. Using the Stefan-Boltzmann radiation equation shown below, and a radiator efficiency of 0.8, a TEC with ΔT of 50°C would be needed for each group to keep the instruments from overheating.

$$Q = \varepsilon\sigma A \left(T_h^4 - T_{\text{amb}}^4 \right) \quad (10)$$

Where Q is the radiated heat power [W], ε is the emissivity of the radiator surface (efficiency), σ is the Stefan-Boltzmann constant, $5.67 \times 10^{-8} \text{ W/m}^2\text{K}^4$, A is the effective surface area of the radiator [m^2], T_h is the temperature of the hot side of the radiator [K], and T_{amb} is the ambient background temperature [K].

F. Attitude Control System

1. ACS Requirements

The attitude control system (ACS) is responsible for determining the attitude of both GALE and AEGIS and administering attitude adjustments via active control hardware to ensure all mission and science requirements are fulfilled. The main requirements for the ACS are presented in Table 29; for the full list of subsystem requirements reference Appendix A.

Table 29 Top-Level Attitude Control System Requirements

ID	Requirement	Rationale
OR-ACS-01	The ACS shall provide attitude knowledge with an error of less than 50 arcseconds	Ensures accurate attitude determination
OR-ACS-02	The ACS shall ensure that both spacecraft maintain a nominal orientation to meet all science requirements and mission objectives	Ensures mission success through fulfilling all objectives
OR-ACS-03	The ACS shall possess a fault-tolerant and redundant design which allows continued operation even with degraded sensors	Ensures some attitude control can be maintained despite degradation/damage
GA-ACS-01	The ACS shall possess three operational modes - a science mode when operating the laser Doppler instrument; a communication mode; and a safe mode (a Sun-pointing configuration)	Provides clear distinction between operating phases and optimizes spacecraft performance
GA-ACS-02	The ACS shall execute reorientation maneuvers within 60 seconds	Ensures quick response time
AE-ACS-01	The ACS shall maintain a controlled descent rate within ± 0.2 m/s for precise landing in Hellas Planitia	Ensures descent rate as determined by orbital requirements is correct
AE-ACS-02	The ACS shall possess three operational modes - a descent mode for attitude control during EDL; a science mode (for optimal science measurements); and a safe mode (to minimize lander exposure to extreme weather)	Provides clear distinction between operating phases and optimizes spacecraft performance
AE-ACS-03	The ACS shall maintain minimal operational capabilities even in the case that primary control elements are lost	Ensures some degree of attitude control can be maintained despite sensor damage
AE-ACS-04	The ACS shall ensure that the lander maintains an appropriate orientation (e.g. within $\pm 1^\circ$ of local gravity) to ensure accurate and nominal operation of science instruments	Ensures science instruments can operate nominally

2. Instruments aboard GALE

On GALE, the ACS will be comprised of four Rocket Lab RW4-12.0 reaction wheels, two Honeywell Miniature Inertial Measurement Units (MIMUs), two Rocket Lab ST-16RT2 Star Trackers, two Redwire Space Fine Pointing Sun Sensors, and eight Aerojet Rocketdyne MR-106L 22N RCS thrusters.

Table 30 Attitude Control System Components aboard GALE

Instrument	Name	Range	Physical Dimensions [†]	Operating Temp (°C)	Power (W)	Mass (kg)	TID [‡]	Qty
RCS Thruster	A-R MR-106L	10–34 N	45 (D) × 200	–	25	0.590	–	8
Reaction Wheel	Rocket Lab RW4-12.0	± 0.2 Nm	264 (D) × 70	−20 – +60	40	5.000	60	4
IMU	Honeywell MIMU	< 375 °/s	234 (D) × 170	−30 – +65	32	4.700	100	2
Star Tracker	Rocket Lab ST-16RT2	3 °/s	99 (D) × 120	−40 – +48	1	0.243	18	2
Sun Sensor	Redwire Space Fine Pointing Sun Sensor	4.25° × 4.25°	150 × 100 × 70	−30 – +60	< 1	2.030	100	2

The IMUs, star trackers, and sun sensors will serve to provide attitude data to the flight computer. This combination is optimal because sensor fusion between each of the instruments will aid in providing the most accurate attitude data possible. Additionally, hardware redundancy will drive down the probability of failure of the attitude control system.

The reaction wheels serve as the primary method of attitude control, and as with most orbiting spacecraft, four of them are used to achieve redundancy if a reaction wheel fails. The RCS thrusters serve as a method of desaturation and momentum dumping for the reaction wheels, should such maneuvers be necessary. Each thruster will be mounted on one of the eight corners of the orbiter to ensure full attitude control. Table 30 lists the components of the ACS aboard GALE.

3. Instruments aboard AEGIS

Table 31 Attitude Control System Components aboard AEGIS

Instrument	Name	Range	Physical Dimensions [†]	Operating Temp (°C)	Power (W)	Mass (kg)	TID [‡]	Qty
RCS Thruster	A-R MR-106L	10–34 N	45 (D) × 200	–	25	0.590	–	8
Inclinometer	NavStar GMS 800	360°	160 × 160 × 100	−40 – +85	–	1.350	–	3
Landing Legs	AEGIS Landing Legs	–	1210 × 30 × 30	–	–	10.000	–	3
IMU	Honeywell MIMU	< 375 °/s	234 (D) × 170	−30 – +65	32	4.700	100	2
Star Tracker	Rocket Lab ST-16RT2	3 °/s	99 (D) × 120	−40 – +48	1	0.243	18	2
Sun Sensor	Redwire Space Fine Pointing Sun Sensor	4.25° × 4.25°	150 × 100 × 70	−30 – +60	< 1	2.030	100	2

[†]All dimensions in mm; [‡]total integrated radiation dose allowable, in krad

On AEGIS, the ACS will be comprised of two Redwire Space Fine Pointing Sun Sensors, two Rocket Lab ST-16RT2 star trackers, two Honeywell MIMUs, three NavStar GMS800 Inclinometers, three adjustable landing legs, and eight

Aerojet Rocketdyne MR-106L 22N RCS thrusters.

The re-entry vehicle, specifically, will employ the RCS thrusters to fine tune its re-entry trajectory, with attitude data acquired via the IMUs, sun sensors, and star trackers. Upon landing, the lander will utilize the three inclinometers to acquire attitude data on the ground and actuate the lander's adjustable landing legs to ensure level operation with respect to local gravity. Table 31 lists the components of the ACS aboard AEGIS.

4. Desaturation Analysis

Given the requirement **OR-ACS-02**, the attitude control system must provide a solution to desaturate GALE's reaction wheels so that the spacecraft can maintain its nominal orientation consistently. As aforementioned, the attitude control system employs the use of eight MR-106L RCS thrusters which will be responsible for desaturating GALE's reaction wheels. **OR-ACS-02.02** states that desaturation shall occur within 10 seconds of firing the RCS thrusters; let's ensure that the thrusters provide enough torque to do so.

Each reaction wheel provides a maximum momentum of 12 Nms, and each thruster can provide anywhere from 10 to 34 N of thrust (with 22 N being nominal). Adjustable thrust levels are key here since with three orthogonal axisymmetric thruster locations (relative to the physical center of the spacecraft), different thrusts are required to ensure full 3-axis desaturation. If each thruster provides the same 22 N of thrust, one axis is essentially locked since the lever arm of the other two axes are equal. Thus, let's simply use an example force vector of $\mathbf{F} = [22, 22, 30]$ N. The distances between each thruster and GALE's center of mass are also known, so it's possible to find the time required to fully desaturate each reaction wheel. Given

$$\mathbf{h}_{\max} = [12, 12, 12] \text{ Nms}$$

$$\mathbf{F} = [22, 22, 30] \text{ N}$$

$$\mathbf{r} = [0.9964, -0.5911, -0.5911] \text{ m}$$

where \mathbf{r} is the distance from the center of mass to any three orthogonally-firing thrusters, the torque generated by each thruster around the center of mass is:

$$\boldsymbol{\tau} = \mathbf{r} \times \mathbf{F}$$

$$\Rightarrow \boldsymbol{\tau} = [-4.729, -42.896, 34.925] \text{ N}$$

Then, to find the time to desaturate each of the wheels at maximum momentum, simply divide the maximum momentum by the calculated torque:

$$t_{\text{desaturate}} = \mathbf{h}_{\max} / \boldsymbol{\tau} \approx [2.5376, 0.2797, 0.3436] \text{ sec}$$

These times are all less than 10 seconds without using maximum thrust, thus fulfilling **OR-ACS-02.02**.

5. Maximum Spacecraft Slew Rate Analysis

Given requirement **GA-ACS-XX (fill in later)**, GALE must be able to slew a minimum of 30 degrees in all axes within two minutes. This ensures that its orientation can be adjusted promptly. To verify if this requirement is met, a simple analysis will be conducted. Given

$$\mathbf{J} = \begin{bmatrix} 2054.1494 & -0.1797 & 201.7285 \\ -0.1797 & 1357.9969 & 0.1022 \\ 201.7285 & 0.1022 & 2491.1962 \end{bmatrix} \text{kgm}^2$$

$$m_{\text{rw}} = 4 \text{ kg}$$

$$r_{\text{rw}} = 0.1285 \text{ m}$$

$$\tau_{\text{rw}} = [0.2, 0.2, 0.2] \text{ Nm}$$

where \mathbf{J} is the spacecraft's moment of inertia tensor with respect to its center of mass and m_{rw} , r_{rw} , and τ_{rw} is the mass, radius, and maximum torque of the RW4-12.0 reaction wheels, let's first calculate the principal moments of inertia (the eigenvalues of the matrix), the axial moment of inertia of the reaction wheels, and the maximum angular acceleration of GALE.

$$\mathbf{J}^* = \begin{bmatrix} 1.3580 & 0 & 0 \\ 0 & 1.9753 & 0 \\ 0 & 0 & 2.5701 \end{bmatrix} \text{kgm}^2$$

$$I_{zz} = \frac{1}{2}m_{\text{rw}}r_{\text{rw}}^2$$

$$\dot{\boldsymbol{\omega}} = \mathbf{J}^{*-1}\boldsymbol{\tau}_{\text{rw}}$$

$$\Rightarrow \dot{\boldsymbol{\omega}} \approx \begin{bmatrix} 0.1473 \\ 0.1013 \\ 0.0778 \end{bmatrix} \text{ mrad/s}$$

With this angular acceleration, let's find the maximum slew possible in 2 minutes:

$$t_{\text{slew}} = 120 \text{ sec}$$

$$\theta = \frac{1}{2}\dot{\boldsymbol{\omega}}t_{\text{slew}}^2$$

$$\Rightarrow \theta \approx \begin{bmatrix} 60.7556 \\ 41.7694 \\ 32.1026 \end{bmatrix} \text{ deg}$$

This fulfills the slew angle requirement outlined in **OR-ACS-02.03**.

6. Pointing Jitter and Accuracy Estimation

A preliminary estimation for pointing jitter and pointing accuracy was also conducted. For pointing jitter, the minimum torque able to be generated by the RW4-12.0 reaction wheels was estimated since a precise value was not given. Industry practices often estimate minimum torques for similar reaction wheels using

$$\tau_{\min} = \frac{\tau_{\max}}{n}$$

where $n \in [10^3, 10^4]$. To estimate pointing jitter, the following equation can be used:

$$PJ \approx \mathbf{J}^{*-1} \tau_{\min} t_{\text{loop}}^2$$

where t_{loop} is the control system's updating time step (estimated as 0.1 seconds here and is typically in the range of 0.1-0.01 seconds). Thus, the pointing jitter is estimated to be

$$PJ \approx \begin{bmatrix} 0.1473 \\ 0.1013 \\ 0.0778 \end{bmatrix} \cdot 10^{-5} \text{ mrad}.$$

This fulfills the pointing jitter requirement outlined in **OR-ACS-02.04**.

For pointing accuracy, a lower-bound value was preliminarily calculated. In theory, pointing accuracy is generally calculated as the root square sum of sensor noise, actuator quantization, and attitude disturbances caused by disturbance torques (i.e. due to gravity gradient, atmospheric drag, etc):

$$PA \approx \sqrt{\theta_{\text{sensor}}^2 + \theta_{\text{actuator}}^2 + \theta_{\text{dist}}^2}$$

To determine a upper-bound value for sensor noise, this is simply the requirement for attitude determination precision (50 arcseconds or 0.9696 milliradians). As for actuator quantization, this is equivalent to the pointing jitter calculated above. For attitude changes caused by disturbance torques, we can simply calculate these as such:

$$\theta_{\text{dist}} \approx \mathbf{J}^{*-1} \tau_{\text{dist}} t_{\text{loop}}^2$$

where $\tau_{\text{dist}} \approx 10^{-5}$ Nm, a typical value used for disturbance torques in orbit. Thus, we can calculate each term:

$$\theta_{\text{sensor}} = 0.9696$$

$$\theta_{\text{actuator}} = PJ$$

$$\theta_{\text{dist}} = \begin{bmatrix} 0.7634 \\ 0.5063 \\ 0.3891 \end{bmatrix} \cdot 10^{-7} \text{ mrad}$$

Seeing as the θ_{actuator} and θ_{dist} are negligible compared to θ_{sensor} , the pointing accuracy in this case is simply approximated

as the sensor noise.

$$PA \approx 0.9696 \text{ mrad}$$

This fulfills the pointing accuracy requirement outlined in **OR-ACS-02.05**.

G. Communications

1. Communications Requirements

Table 32 Top-Level Communications System Requirements

ID	Requirement	Rationale
OR-COMM-01	The communication subsystem shall be responsible for the transmission of data between spacecraft and with Earth groundstations	Ensures successful transmission of data to Earth
OR-COMM-02	The communications subsystem shall have redundant design capable of nominal operation in the event of single component failure	Fault tolerant design enables successful mission in the event of component failures
GA-COMM-01	The GALE communications subsystem shall be capable of receiving 2.94 kbps of data centered at 401 MHz	Based on the amount of data collected on the AEGIS craft and time available to transmit
GA-COMM-02	The GALE communications subsystem shall be capable of transmitting 1.4 Mbps of data centered at 8425 MHz with a gain of at least 75 dB	Minimum gain to account for maximum losses in transmission to Earth
GA-COMM-03	The GALE spacecraft shall be capable of storing 200 Gb of data	Enables one week of data storage in the event of an anomaly and temporary loss of communications
AE-COMM-01	The AEGIS communications subsystem shall be capable of transmitting 2.94 kbps of data centered at 401 MHz	Based on the amount of data collected and time available to transmit
AE-COMM-02	The AEGIS spacecraft shall be capable of storing 400 Mb of data	Enables two days of data storage in the event of temporary communications loss.

The communications subsystem is responsible for the transmission of data between spacecraft and down-linking all acquired data to Earth for processing and dissemination. As such, the communications system is vital to the success of the mission; a failure of the communications system would result in a failure to complete the mission. For the most part, the communication requirements stem from the constraints of other subsystems. With the amount of power available limited by storage and production capability, the gain of the communications system is limited. Additionally, the orbit designed to achieve all scientific objectives poses challenges and further constrains the communication system operation. Having only 16 minutes of line of sight for communications per day, the link between the AEGIS lander and GALE orbiter must be able to store all data acquired throughout the day and transmit that data during the available ground passes. The required amount of data is driven by the time of operation per day of each instrument. Some thermal

considerations must be taken into account to ensure nominal operations of all communications components, allowing for efficient and complete transmission of all scientific and telemetry data generated during the mission.

2. AEGIS to GALE

Based on current estimates of data generated by each instrument aboard the AEGIS lander, approximately 196.6 Mb of data is generated for transmission per day. Including a 15% overhead for 223/255 Reed-Solomon encoding, the total data transmitted per day will be 226.1 Mb. With only 16 minutes of ground passes available for transmission to the GALE orbiter per day, where a ground pass is defined as having line of sight between craft 20° above the horizon, the necessary Communication Throughput Rate (CTR) is 2.94 Kb/s including telemetry data, encoding, and a 25% growth margin. This ground pass time estimate comes from the polar sun synchronous science orbit of the GALE craft.

The link between craft consists of a transceiver, medium gain antenna on the lander, low gain antenna on the orbiter, and transceiver on the orbiter. Between lander and receiver, the radiated signal loses power to free space and limited power to the thin martian atmosphere. The radio will use the UHF band, operating at 401 MHz with a bandwidth of 15 MHz, QPSK modulation scheme, and right-hand polarized signal. UHF ensures that communication with the orbiter remains even in high loss conditions such as dust storms while also being high enough frequency to accommodate the large data rate necessary to transmit all data to the orbiter during the 16 minutes of daily ground-passes.

To close the link between lander and orbiter, the transceiver power and antenna sizes were iterated to achieve a low-mass, low-power system. Limited to 10W of power, A 0.25-meter diameter parabolic antenna is used to point transmission to the orbiter where low-gain antennas pointing in each axis facing towards or parallel to the Martian surface can passively receive transmission without the need for special maneuvers or control. The overall link budget for the lander can be found in table 33. This high SNR allows for high bandwidth transmission and ensures large margins in the event of dust storms or non-optimal pointing.

Table 33 Link budget required to transmit telemetry and scientific data between craft and to Earth using DSN receivers

	AEGIS to GALE (dB)	GALE to Earth (dB)
Supplied Power	40.00	50.00
Antenna Gain	3.41	45.47
Free Space Loss (max)	-177.90	-283.02
Atmospheric Loss (max)	-0.50	-4.71
Pointing Loss (max)	-2.40	-12.20
Receiver Gain	1.64	74.18
Noise	-153.83	-155.59
SNR	18.84	23.76

Table 34 Data generated for transmission per instrument on each spacecraft

Spacecraft	Instrument	Data Transmission Rate (Kbps)	% Operation per Hour
GALE	Laser Doppler Wind Lidar	8	25%
	Reconnaissance Imaging Spectrometer	400	75%
	Infrared Radiometer	100	7%
	Subsurface Radar Sounder	26	50%
Total Acquired Per Day:		27.9 Gb	
AEGIS	Saltation Sensor	0.320	25%
	Radiation Assessment Detector	0.273	25%
	Imaging Cameras	0.173	2.5%
	Thermo(pile/couple)	0.639	8.3%
	Pressure Transducer	0.213	8.3%
	2D wind sensor	0.213	8.3%
	MicroARES Electric field sensor	1.280	2.5%
	Solar Irradiance Sensor / Flux Radiometer	0.020	12.5%
	Laser Doppler dust velocimeter/anemometer	8	25%
Total Acquired Per Day:		197 Mb	

3. GALE to Earth

The GALE orbiter must be able to transmit both the data generated by the AEGIS lander and all the data generated onboard the GALE craft shown in Table 34. Large free space losses from Mars to Earth require the use of the Deep Space Network to communicate with the GALE spacecraft, limiting frequency bands to those supported by the DSN; L-band, S-band, X-band and Ka-band [7]. Balancing between the larger free space losses that come with higher frequencies and the larger data rates that those higher frequencies bring, X-Band communications are suitable to close the link between the GALE spacecraft and the DSN with large margins to account for non-ideal losses not fully accounted for in link budget development shown in Table 33. A 3 meter diameter parabolic antenna is used to point transmission from Martian orbit to Earth, where it is received on 34m DSN antennas located in Canberra, Australia; Madrid, Spain; and Goldstone, CA, United States, allowing for nearly continuous communications if needed. For this mission, due to orbital parameters, the GALE craft will have a line of sight with Earth for at least 75% of each day, though for power and monetary budgeting constraints, only 8 hours per day are allocated for communications. This value is used to determine the required CTR with a margin of 1.40 Mb/s after Reed-Solomon 223/255 encoding consistent with DSN encoding requirements [8]. To achieve this data rate, the radio uses an X-band frequency of 8425 MHz with a bandwidth of 3 MHz, QPSK modulation scheme, and right-hand polarized signal.

Time receiving on the Deep Space Network's 34m antenna costs approximately \$1691 per hour according to NASA's Mission Operations and Communications Services guide [8]. During the cruise phase to Mars, the spacecraft will link with the ground station every other day to confirm trajectory and health of the spacecraft. Upon reaching Mars, the spacecraft will begin the aerobraking phase where the GALE craft will communicate with the ground after every

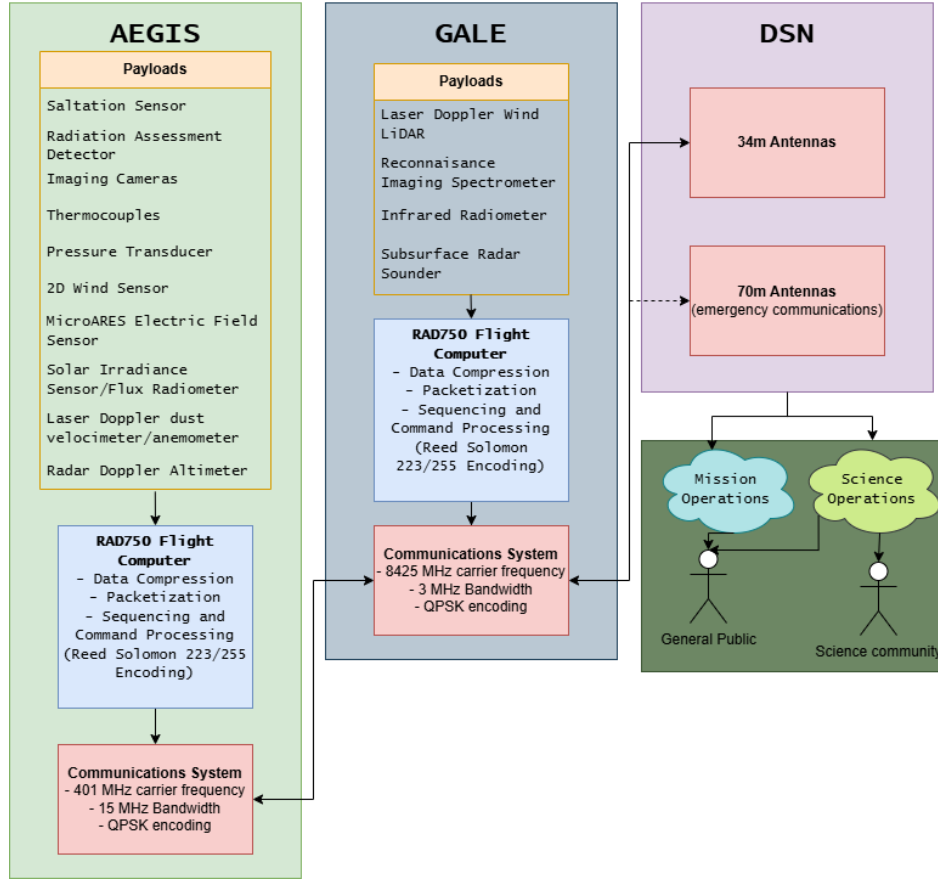


Fig. 21 Mission Data Flow Diagram

aerobraking pass to ensure the health of the vehicle. Once reaching science orbit, the vehicle will link with ground stations daily to transmit all accumulated science and health data to the science operations center for processing and dissemination to the scientific community and public. During the primary mission phase, the maximum delay in communicating with Earth ground stations is 22 minutes, or 44 minutes round trip, this means that all operations must be fully autonomous and safe operational modes must allow for communication with Earth even without any operator input.

4. Data Budget

An overview of the data flow architecture can be found in Figure 21 this summarizes the communication paths between both spacecraft and to Earth. A typical day in the life data budget for the AEGIS and GALE craft can be found in Tables 35 and 36 highlighting the amount of data acquired and transmitted every hour of throughout the day. It can be seen that all desired data during typical operation can be fully stored and transmitted between craft and to Earth.

Table 35 Typical Day in the Life Data budget of the AEGIS Spacecraft

(Hour)	Mode	Data Generated (Mb)	Data Downloaded (KB)	Mass Storage Balance (Mb)	Available Space on Mass Storage (Mb)
0	Nominal	8.2	0	-8.2	400
1	Nominal	8.2	0	-8.2	391.8
2	Nominal	8.2	0	-8.2	383.6
3	Nominal	8.2	0	-8.2	375.4
4	Nominal	8.2	0	-8.2	367.2
5	Nominal	8.2	0	-8.2	359
6	Nominal	8.2	0	-8.2	350.8
7	Nominal	8.2	0	-8.2	342.6
8	Nominal	8.2	0	-8.2	334.4
9	Nominal	8.2	0	-8.2	326.2
10	Nominal	8.2	0	-8.2	318
11	Nominal	8.2	0	-8.2	309.8
12	Data Transmit	8.2	0	89.8	399.6
13	Nominal	8.2	0	-8.2	391.4
14	Nominal	8.2	0	-8.2	383.2
15	Nominal	8.2	0	-8.2	375
16	Nominal	8.2	0	-8.2	366.8
17	Nominal	8.2	0	-8.2	358.6
18	Nominal	8.2	0	-8.2	350.4
19	Nominal	8.2	0	-8.2	342.2
20	Nominal	8.2	0	-8.2	334
21	Nominal	8.2	0	-8.2	325.8
22	Nominal	8.2	0	-8.2	317.6
23	Nominal	8.2	0	-8.2	309.4
24	Data Transmit	8.2	0	89.8	399.2

Table 36 Typical Day in the Life Data budget of the GALE Spacecraft

(hour)	Mode	Data Generated (Gb)	Data Downloaded (Mb)	Mass Storage Balance (Gb)	Available Space on Mass Storage (Gb)
0	Nominal	1.16	0	-1.16	200
1	Nominal	1.16	0	-1.16	198.84
2	Nominal	1.16	0	-1.16	197.68
3	Nominal	1.16	0	-1.16	196.52
4	Nominal	1.16	0	-1.16	195.36
5	Nominal	1.16	0	-1.16	194.2
6	Nominal	1.16	0	-1.16	193.04
7	Nominal	1.16	0	-1.16	191.88
8	Nominal	1.16	0	-1.16	190.72
9	Nominal	1.16	0	-1.16	189.56
10	Nominal	1.16	0	-1.16	188.4
11	Nominal	1.16	0	-1.16	187.24
12	Data Receive	1.16	-98	-1.16	185.982
13	Nominal	1.16	0	-1.16	184.822
14	Nominal	1.16	0	-1.16	183.662
15	Nominal	1.16	0	-1.16	182.502
16	Nominal	1.16	0	-1.16	181.342
17	Nominal	1.16	0	-1.16	180.182
18	Data Transmit	1.16	0	2.29	182.472
19	Data Transmit	1.16	0	2.29	184.762
20	Data Transmit	1.16	0	2.29	187.052
21	Data Transmit	1.16	0	2.29	189.342
22	Data Transmit	1.16	0	2.29	191.632
23	Data Transmit	1.16	0	2.29	193.922
24	Data Transmit/Receive	1.16	-98	2.29	196.114

launch vehicle, insurance, propellant and logistics cost. Most of the cost is related to the Falcon Heavy which is \$200 million dollars, one fifth of our budget. The launch vehicle combined with project development equates to a total of \$343,790,000 for the launch and transit section. The GALE spacecraft accounts for a total of \$136,186,576 with the majority of that coming from payloads and the LiDAR. The spacecraft has all the necessary subsystems required for nominal operations with a average cost margin of 10% to 20% applied to each subsystem. The AEGIS lander accounts for almost half of the entire budget with a total of \$459,839,396. The two elements the increase the cost the most is the Entry Decent and Landing (EDL) system and the Radioisotope Thermoelectric Generator (RTG). Similar to the GALE the a cost margin of 10% to 20% was added to all subsystem components with a few exceptions for landing legs and main thruster. In total the ORACLES mission is \$939,815,971 with approximately \$60 million under the 1 billion dollar budget.

As for the mass budget, Figure 22 also shows the estimated device masses, mass growth allowance, and predicted mass per device unit. A summed mass for both the GALE orbiter and AEGIS lander is calculated, where GALE is approximately 1848 kilograms and AEGIS is about 1747 kilograms. Since many, if not all of the instruments and devices onboard the spacecraft have specifically defined masses, a 10% growth allowance was used to account for any necessary changes to each device to be functional on either spacecraft. On the GALE orbiter, the structures contributes the largest to the total mass at 663kg. The DAWN wind doppler Lidar contributes the largest percentage of the instrument mass at 450kg. Other devices contributing the next highest percentage of instrument mass are the spectrometer and X-band high gain antenna at roughly 33kg each, and other subsystem devices contribute a significantly smaller amount of mass to the overall mass of the orbiter. On the lander, the re-entry vehicle, structure, and lander propulsive system contribute the most mass at 719kg, 267kg and 200kg, respectively. All other devices are significantly less mass, with the radar altimeter contributing 70kg and MMRTG contributing 45kg to the total mass. All other instruments and devices have individual masses of less than 20kg. After growth allowances and summing the total mass of both GALE and AEGIS, the total mission mass is calculated to be 3596 kilograms. This calculated mass falls well below the estimated mass the launch vehicle (Falcon Heavy) can deliver to Mars (nearly 17000 kilograms).

B. Risk Analysis

Figure 37 shows the likelihood consequence matrix for the most critical failure probabilities across the entire mission, and table 37 describes each risk and top level explanations to mitigate each risk. Table 38 provides a legend to describe each risk on the likelihood consequence diagram as either a mission risk, subsystem level risk or device/instrument level risk. While none of the risks to the mission have an estimated likelihood of happening above 51 percent, risks such as M.1 (EDL risks) and S.1-3 (thermal, propulsive, and power risks) are catastrophic to the mission should they fail. Therefore, associated mitigation strategies for each risk are identified and explained in further detail.

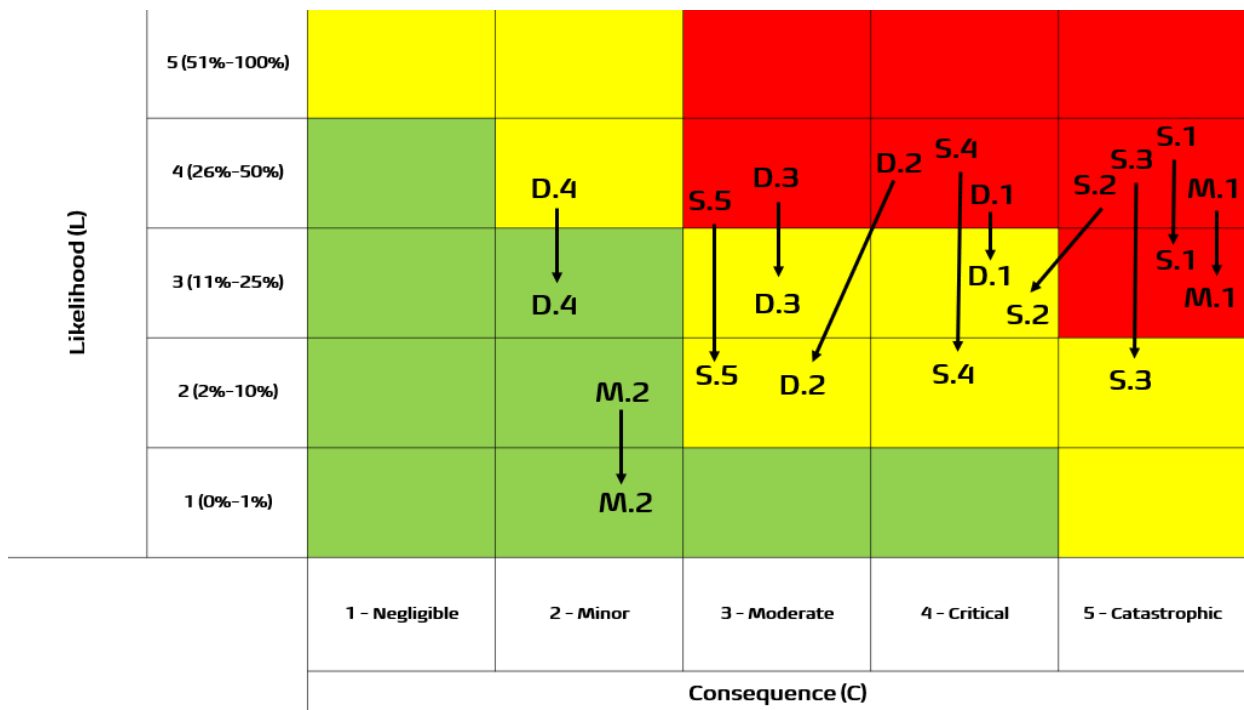


Fig. 23 Likelihood-Consequence risk matrix.

Table 37 Risk Register

Risk ID	Risk Description	Mitigation
M.1	If the spacecraft is damaged or lost during EDL, the mission fails as a whole.	Full-fidelity EDL simulations of aerobraking and AEGIS descent under nominal entry conditions.
M.2	If the spacecraft cannot launch on Dec. 31, 2028, the mission will miss its launch-date goal.	Evaluate multiple contingency launch windows in case of developmental delays.
S.1	If Thermal Control System or RTG fails, instruments and subsystems overheat or freeze.	Design redundant TCS loops and backup heaters to isolate single-point failures.
S.2	If any propulsion engine loses thrust, 6-DOF control may be lost, risking mission loss.	Implement engine-level redundancy and cross-strapped feed lines; include multiple engines.
S.3	If electrical power generation/storage fails, all dependent systems go offline.	Provide redundant power strings and automatic reconfiguration upon failure.
S.4	If communications link to Earth is lost, no science data can be returned.	Include redundant dual-band transceivers and deployable high-gain antenna as backup.
S.5	If Attitude Control System fails, pointing/navigation degrade to monopropellant control only.	Cross-strap reaction wheels, include backup IMUs and thruster hot-spares for attitude control.
D.1	If electrodynamic dust discharge (EDD) fails, solar panels foul with dust, reducing power.	Continue EDD R&D; add mechanical wipers and redundant electrode arrays.
D.2	If DAWN orbiter instrument ALADIN fails on deployment, key science data are lost.	Joint development/testing with ESA and ALADIN manufacturer; high-fidelity deployment tests.
D.3	If AEGIS lander's primary instruments fail to deploy, critical surface data are lost.	University-led TRL-advancement program and full-cycle deployment drills.
D.4	If AEGIS lander's secondary instruments fail, auxiliary science return is compromised.	Partner with instrument vendors for enhanced quality control and in-flight functional checks.

Table 38 Risk Classification Legend

Prefix	Classification
M	Mission-level risk
S	Subsystem-level risk
D	Device-/instrument-level risk

1. EDL Analysis

Inaccurate modeling of entry, descent, and landing aerodynamics—due to uncertainties in Mars’s atmospheric density profile, vehicle aerothermal loads, or parachute dynamics can lead to underestimating deceleration, thermal soak or stability margins. This poses a risk on structural failure and in turn, loss of the lander. Even small errors in drag coefficient or heat shield performance can lead to suboptimal aerobraking and descent trajectories, which have the capability to have catastrophic consequences.

Mitigation combines extensive high-fidelity simulation with hardware-in-the-loop validation. Coupled computational fluid dynamics and monte carlo simulation models can be executed across multiple Martian atmospheric profiles, then

validated against Mars entry wind tunnel tests. Subscale drop tests and parachute-inflation trials will calibrate drag coefficients and stability predictions. Redundant pressure ports, inertial measurement units, and altimeters will feed a closed-loop guidance, navigation, and control algorithm in addition to the primary sensors that will continuously adjust the descent trajectory in real time.

2. Orbit Analysis

Errors in orbit propagation arising from imperfect Mars gravity models, solar radiation pressure, or unmodeled third-body effects can lead to incorrect insertion burns, station-keeping maneuvers, or phasing for lander deployment. Errors in navigation bias or incorrect ΔV can also result in suboptimal orbits and fuel exhaustion, which can pose a threat to the mission should the error be sufficiently high.

Precision modeling and real-time correction will be done to reduce any risks during transit and orbit around Mars. An ensemble propagation system merges up-to-date Mars gravity and atmospheric drag models with solar radiation pressure and third-body perturbations, each calibrated against telemetry from previous orbiters. Onboard orbit determination relies on radiometric tracking and optical-landmark recognition to refine state estimates. Periodic, covariance-based trajectory-correction maneuvers guided by Monte Carlo sensitivity analyses will also secure robust margins for insertion, station-keeping, and phasing during the course of the mission.

3. Orbiter Instrument Analysis

Failure of any GALE orbiter instrument would critically undermine the mission's scientific return. Should instruments such as the subsurface radar sounder or the wind doppler lidar fail, the volume of atmospheric and geological resource data will be significantly reduced, which could lead to an overall mission failure.

Technical partnerships with ESA and leading academic labs will drive the necessary design iterations—downsizing from the ALADIN baseline, hardening for lower temperatures, and in-orbit functional testing—to mature DAWN from TRL 4–5 to TRL 6–7 before launch. Lessons learned from CRISM and the Mars Climate Sounder on prior missions will inform deployment-sequence adaptations, thermal and data-handling interface refinements, and performance validation in simulated GALE-orbit conditions for both the compact imaging spectrometer and MCS (each at TRL 8).

University research teams and the NASA/ESA Mars Express MARSIS coordinators will be engaged to tailor the subsurface radar sounder's signal-processing and feature-detection algorithms for Hellas Planitia. In-flight performance data from MARSIS, combined with ground-based deployment drills, will ensure reliable detection of ice deposits and lava-tube signatures, thereby mitigating the remaining development risk.

4. Lander Instrument Analysis

Similar to the orbiter, if any critical science instrument on AEGIS fails, the overall scientific yield will be notably reduced. To reduce the risk of failure, pre-mission testing in Mars-analog pressure and temperature chambers will advance the TRLs of the saltation sensor and dust anemometer through thermal-vacuum cycling, dynamic wind-tunnel trials, and dust-grain transport simulations. Collaboration with researchers specializing in aeolian dynamics and benchmarking against InSight and Curiosity datasets will guide calibration protocols and performance validation for both the electric field sensor and flux radiometer under simulated Martian dust-charging conditions.

Flight-proven thermopiles, pressure transducers, 2D wind sensors, RAD, imaging cameras, radar Doppler altimeter, aerothermal sensor suite, and descent cameras will undergo lander-level integration tests—vibration, thermal-vacuum, and electromagnetic interference/capability—to verify mechanical, thermal, and electrical interfaces within the AEGIS configuration. End-to-end operational demonstrations in Mars-analog environments will confirm sensor sensitivity and data throughput to ensure reliable performance throughout descent and surface operation.

5. Thermal System Analysis

Thermal control is critical to ensure all instruments are able to operate and survive throughout the different phases of the mission. The major risk associated with this is the potential failure of active heating or cooling hardware, which could result in instruments exiting their operating—or worse, survival—temperature ranges.

An additional risk introduced due to design choices is the possibility of wide-scale failure due to instrument groupings. In order to keep the thermal control system as sleek and efficient as possible, instruments with similar operating temperature ranges were grouped together on both the orbiter and the lander. With these groupings, if thermal hardware were to fail in a way that impacts the system’s ability to maintain the required temperature range, this would affect not just a single instrument, but all instruments in that group.

To mitigate this and ensure confidence in system reliability, hardware that is either space-grade or has flight heritage from previous missions was prioritized in the selection process. Additionally, multiple layers of redundancy have been incorporated into the thermal design. Each thermal control system includes a combination of active heating and cooling elements, insulation, and radiative features to ensure that instrument temperatures are consistently regulated.

6. Power System Analysis

A total bus failure from either a battery cell fault, solar-array string loss, or regulator malfunction cuts off electrical power to avionics, instruments, heaters, and propulsion valves. This will halt all spacecraft functions, resulting in spacecraft loss and mission failure.

Dual power strings (fully separate solar arrays, regulators, and battery banks) can feed two independent buses. On-board power-management units will detect under-voltage or over-draw conditions and instantaneously reconfigure

bus ties. Intelligent load-shedding algorithms prioritize critical avionics and thermal loads to ride through partial failures while maintaining minimal survivability.

7. Communication System Analysis

Any loss of uplink or downlink severs data and telemetry paths. Since Mars is at most 400 million km away from Earth, any failure in the communications system would mean a loss of the mission. Therefore, the communications system was designed such that every powered component has a backup and are cross strapped such that a failure of any one component does not result in loss of communications with the spacecraft. Since there is only one HGA onboard the GALE craft, this is the largest source of risk in the communications system. A failure in the HGA actuator would cause large pointing losses and would require modified operations to point the antenna towards Earth by pointing the entire spacecraft. The UHF LGAs onboard GALE do not have strict pointing requirements. Likewise, the .25 m parabolic antenna onboard AEGIS is not fault tolerant, losing the actuation on the antenna would likely mean loss of communications with the lander.

8. Propulsion System Analysis

Failure of any main or auxiliary engine threatens six-degree-of-freedom control: attitude, trajectory corrections, and descent maneuvers become impossible if thrust is lost, leading directly to mission loss. Even a single-point valve or feed-line failure can disable an entire engine, removing critical maneuver capabilities during EDL or orbital insertion.

To mitigate the risk of losing an engine, multiple engines could operate in hot-standby configuration, each with independent propellant lines, valves, and pressure regulators. Automated health monitoring isolates and vents a failing engine without contaminating shared plumbing. Cross-strap manifolds can allow any remaining engine to draw from any feed tank, preserving thrust capability even after a hardware fault.

9. ACS System Analysis

An ACS failure degrades pointing accuracy for solar arrays, antennas, and instruments such as the wind doppler lidar and radar sounder; without fine-point control, the spacecraft must resort to coarse monopropellant pulses, risking rapid propellant depletion, misalignment, and loss of mission objectives.

Redundant reaction-wheel assemblies (each motor and electronics board duplicated) and multiple inertial-measurement units provide overlapping attitude reference. A backup set of monopropellant thrusters could be added with the intention of being reserved exclusively for attitude recovery. Onboard fault-detection and state-estimation software will automatically shift control into the healthiest actuator chain, preserving precise pointing and navigation even after a component fault.

C. Scheduling

Figure 24 presents the end-to-end development timeline for the ORACLES mission, spanning from mission conception in early 2025 through launch, surface deployments, and final decommissioning in 2038. Each horizontal bar corresponds to a specific task or subsystem activity, organized into sequential project phases (Pre-A through E) and punctuated by technical reviews and milestones that guide the project from initial planning to disposal readiness.

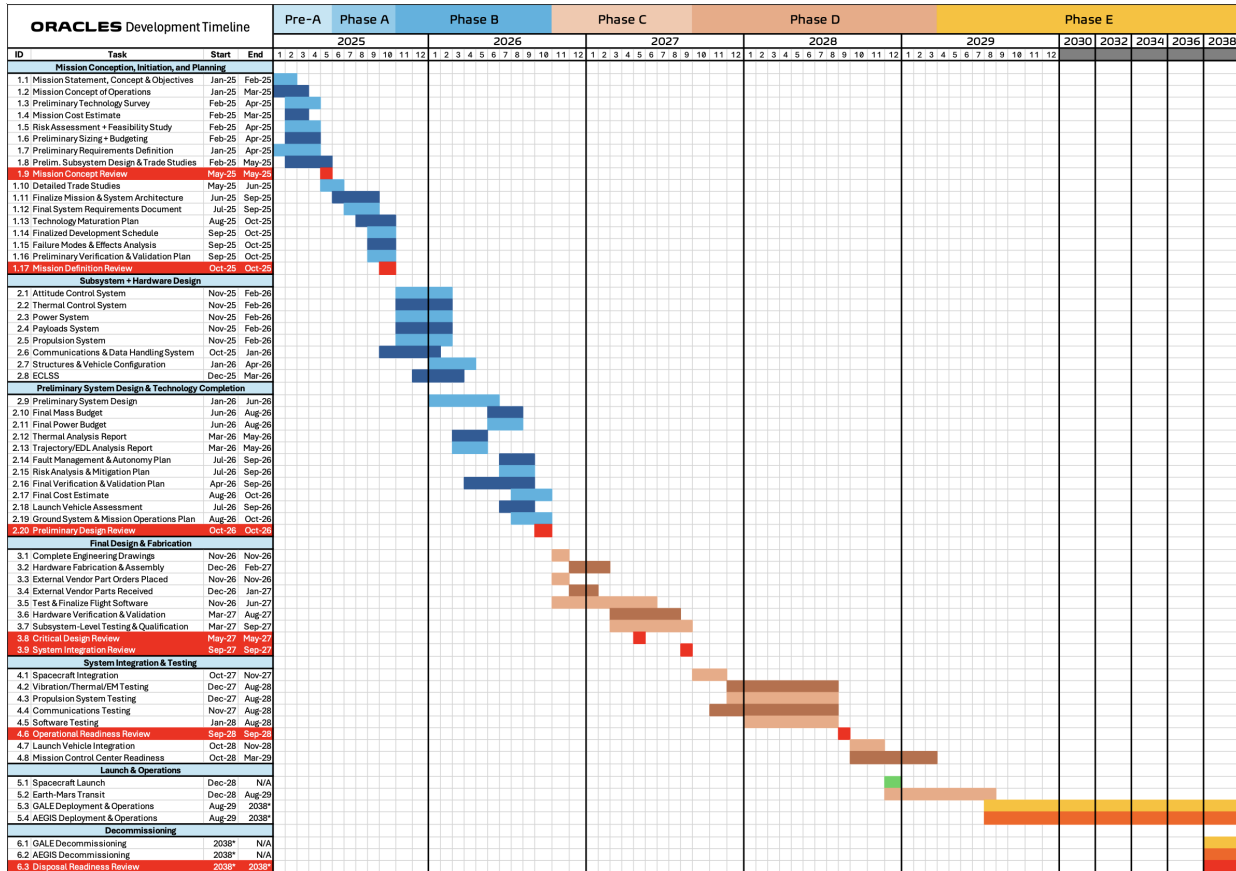


Fig. 24 ORACLES Proposed Mission Schedule.

The ORACLES development timeline spans roughly 15 years, from initial concept work in 2025 through spacecraft decommissioning in 2038. It is organized into five major phases—Pre-A (Concept & Initiation), Phase A (Preliminary Design), Phase B (Preliminary System Design Completion), Phase C (Final Design & Fabrication), Phase D (System Integration & Testing), and Phase E (Launch & Operations)—each punctuated by formal reviews (Mission Concept Review, Mission Definition Review, Preliminary Design Review, Critical Design Review, System Integration Review, Operational Readiness Review, and Disposal Readiness Review). Early tasks (ID 1.1–1.17) cover mission objectives, cost estimating, feasibility studies, requirements definition and trade studies; by October 2025 the Mission Definition Review marks the transition into detailed subsystem design.

During Phase A and B (late 2025 through October 2026), each major subsystem—attitude control, power, thermal,

communications, propulsion, payloads, structures, vehicle configuration and ground operations—is fleshed out in parallel. Key deliverables include the Final Mass & Power Budgets, Thermal and Trajectory/EDL Reports, Fault Management Plan, Risk Analysis & Mitigation Plan, and Ground Systems & Mission Operations Plan. A Preliminary Design Review in October 2026 confirms readiness to flow down requirements into hardware and software.

Phase C (November 2026–May 2027) focuses on detailed engineering drawings, hardware fabrication, part acquisition from manufacturers, and the first-pass flight software builds. The end of Phase C and the completion of the aforementioned tasks is marked by the Critical Design Review in May 2027. Phase D (late 2027 through mid 2028) is dedicated to spacecraft assembly, environmental and propulsion testing of instruments and subsystems, software integration, and culminates in the Operational Readiness Review in September 2028. The launch of the mission will mark the beginning of Phase E on December 31, 2028. This is followed by the Earth-Mars transit, and deployment of GALE and AEGIS after the six month aerobraking period upon Mars arrival. Operation of each spacecraft will last through at least 2038, at which point the Disposal Readiness Review and system decommissioning activities formally close out the mission.

VII. Conclusion

The ORACLES mission answers the call to characterize the Martian environment, doing so from orbit and in situ, in order to prepare for future human exploration on the Red Planet. This tandem approach sees the mission orbiter, GALE, investigate subsurface water deposits and aeolian dynamics, furthering current studies and bringing originally Earth-bound technologies to the Martian atmosphere. Meanwhile, the mission lander, AEGIS, benefits from landing in the lowest basin to collect local data on a dust storm source point and a promising location for human habitation. The associated risks reflect the ambitious mission ORACLES has set forth. Each subsystem underwent rigorous trade studies, constrained by mission requirements and subsystem interdependencies, in order to achieve the most optimal results, minimizing mass and cost while maximizing data collection and mission duration. As a product of the established risk mitigation strategies and concurrent subsystem development, ORACLES is enabled to provide a more complete picture of the Red Planet and facilitate human exploration.

A. Complete Requirements List

A. Orbital Requirements

Table 39 Orbital Requirements

ID	Requirement	Rationale
GA-ORB-01	Delta-V usage of GALE shall be less than then 2 km/s.	Increase fuel and therefore operational lifetime of the mission.
GA-ORB-02	The GALE spacecraft must be in a Martian sun-synchronous 378 km orbit by January 1st 2031.	This is to allow for the gathering of science data by 2033 and the spacecraft should be able to maintain 75% orbital coverage.
GA-ORB-03	The GALE spacecraft periapsis shall be between 100 km and 120 km for aerobraking to lower its orbit.	This is to comply with requirement GA-ORB-01 to minimize delta v usage.
GA-ORB-04	The orbiter shall separate from the lander four days before before the Mars capture burn.	This is to comply with requirement GA-ORB-01 to minimize delta v usage.
AE-ORB-01	Lander shall land in Hellas Planitia located within a 100 km radius of 42.4° South latitude and 70.5° East longitude.	This is a science requirement.
AE-ORB-02	During Entry Decent and Landing AEGIS utilize a direct descent trajectory where the periapsis must be below 20 km in altitude.	This is a functional requirement.
AE-ORB-03	Delta-V usage of AEGIS shall be less than then 1 km/s.	This is to comply with AE-ORB-01.

B. Structures and Configuration Requirements

Table 40 Structures and Configuration Requirements

ID	Requirement	Rationale
OR-STR-01	The spacecraft shall survive the launch environment of the Falcon Heavy Launch Vehicle.	Mission should reach destination in proper form.
OR-STR-01.01	The GALE orbiter primary structure shall withstand, without permanent deformation, static loads equivalent to [4] g's in the longitudinal direction and [2] g's in the lateral directions, combined with a dynamic load factor of [1.5].	Ensures structural integrity during launch; Longitudinal (4 g's): primary thrust axis at Max-Q; Lateral (2 g's): estimate for wind gusts and steering maneuvers; Dynamic Load Factor (1.5): accounts for vibrations and transient loads.
OR-STR-01.02	The AEGIS lander structure, including the EDL components, shall withstand, without permanent deformation, static loads equivalent to [4] g's in the longitudinal direction and [2] g's in the lateral directions, combined with a dynamic load factor of [1.5].	Ensures structural integrity during launch; Longitudinal (4 g's): primary thrust axis at Max-Q; Lateral (2 g's): estimate for wind gusts and steering maneuvers; Dynamic Load Factor (1.5): accounts for vibrations and transient loads.
OR-STR-01.03	The launch vehicle adapter shall withstand, without permanent deformation, the combined static and dynamic loads of the GALE orbiter and AEGIS lander during launch, up to a total axial load of [55] kN.	Ensure structural integrity and payload safety during launch. This number is approximated from the same logic as above requirements, and the equation $1250\text{kg} * 4g * 9.81\text{m/s}^2 = 49kN$, plus margin = 55kN.
OR-STR-02	The spacecraft frame shall provide structural support for all subsystems and instruments during all mission phases.	All instruments and subsystems need to be fairly accommodated for their needs within the design.
OR-STR-02.01	The GALE orbiter structure shall provide mounting interfaces for all subsystems (power, propulsion, communication, etc.) with a combined mass of [350] kg, maintaining a structural safety factor of at least [1.5].	Ensures the orbiter can carry all necessary equipment safely, based on previous mission analysis and adaptation.
OR-STR-02.02	The GALE orbiter primary structure shall maintain its shape and dimensions within a tolerance of [2] mm under operational thermal conditions, ranging from [-150] °C to [100] °C.	Ensures structural stability under thermal variations in space; Tolerance (± 2 mm): reasonable for the structure; Temperature Range (-150 °C to +100 °C): covers Mars orbit extremes.

Table 41 Structures and Configuration Requirements

ID	Requirement	Rationale
OR-STR-02.03	The AEGIS lander structure shall provide mounting interfaces for all subsystems (power, communication, science instruments, etc.) with a combined mass of [150] kg, maintaining a structural safety factor of at least [1.5].	Ensures the lander can carry all necessary equipment safely, based on previous mission analysis and adaptation.
OR-STR-03	The spacecraft shall enable the separation of the GALE orbiter and the AEGIS lander during Mars transfer.	The mission has components with different destinations, but will be packed together for launch.
OR-STR-03.01	The launch vehicle adapter shall incorporate a separation mechanism capable of releasing the AEGIS lander with a separation velocity of $[0.5] \pm [0.1]$ m/s and an angular separation rate not exceeding [2] deg/s.	Ensures controlled and safe separation of the lander; Separation Velocity (0.5 ± 0.1 m/s): typical for spacecraft deployments; Angular Rate (2 deg/s): limits rotation to prevent tumbling.
OR-STR-03.02	The GALE orbiter structure shall withstand the reaction forces from the separation mechanism without exceeding a stress level of [150] MPa.	Ensures separation doesn't damage the orbiter or otherwise inhibit its operation.
OR-STR-03.03	The AEGIS lander structure shall withstand the reaction forces from the separation mechanism without exceeding a stress level of [150] MPa.	Ensures separation doesn't impair the lander or increase landing failure risk.
OR-STR-04	The combined dry mass of structural subsystems, including the launch vehicle adapter, shall not exceed 1250kg.	Based on previous missions of similar architecture and/or goals.
OR-STR-04.01	The GALE orbiter structure shall have a mass not exceeding 750 kg.	This is based on historical comparison and adjusting for new mission goals.
OR-STR-04.02	The AEGIS lander structure shall have a mass not exceeding 450 kg.	This is based on historical comparison and adjusting for new mission goals
OR-STR-04.03	The Launch Vehicle Adapter structure shall have a mass not exceeding 50 kg.	This is based on historical comparison and adjusting for new mission goals
GA-STR-01	Structures & Mechanisms shall accommodate four operational configurations corresponding to operational stages of the mission: Launch, Transit, Aero-braking, and Nominal Operations.	Each of these mission stages will have differing relative orientations to Earth & Sun, and differing key requirements necessitating configurational differences.

Table 42 Structures and Configuration Requirements

ID	Requirement	Rationale
GA-STR-01.01	GALE shall incorporate articulating mechanisms to accommodate the deployment and orientation of solar panels and communication antennas.	To enable GALE to achieve its operational goals for power generation and communication by allowing proper orientation of solar panels and antennas, which necessitates articulating mechanisms supported by the spacecraft structure.
AE-STR-01	Lander structures shall accommodate three configurations: Stowed, Landing, and Nominal Operations.	Each of these mission stages have differing key requirements necessitating configurational differences.
AE-STR-01.01	AEGIS shall incorporate articulating mechanisms to accommodate the deployment and orientation of solar panels and communication antennas.	To enable AEGIS to achieve its operational goals for power generation and communication by allowing proper orientation of solar panels and antennas, which necessitates articulating mechanisms supported by the lander structure.
AE-STR-01.02	AEGIS shall have an articulating mechanism for its landing legs to allow for stowing during transit and deployment for landing.	To allow the landing legs to be retracted during transit and deployed for landing, providing a stable and level platform for AEGIS on the Martian surface.
AE-STR-02	Lander shall have landing legs that maintain a level platform, and support the structure.	Equipment onboard lander requires a secure platform, instruments require a steady and level platform.
AE-STR-02.01	The AEGIS lander shall achieve a level orientation within ± 1 degree on slopes up to 15 degrees after landing.	AEGIS's instruments and operations require a stable and level platform on the Martian surface for accurate data collection and proper functioning.
AE-STR-02.02	AEGIS shall meet a stability requirement on the Martian surface once landed.	AEGIS needs to remain stable on the Martian surface to ensure the safety and functionality of its instruments and overall operations, preventing tipping or unwanted movement.

C. Power Requirements

Table 43 Power Requirements and Rationale

ID	Requirement	Rationale
GA-POW-01	The EPS shall deliver enough power to support duty cycles in excess of 75% across all four scientific instruments.	Ensures sufficient coverage and flexibility for various investigations, within a minimized risk.
GA-POW-02	The EPS shall be capable of delivering 1013.1 W in an operation power cycle.	Ensures enough power to operate scientific instrumentation, handle data, and maintain temperature and orbit.
GA-POW-03	The EPS shall be capable of delivering 1553.9 W in a peak power cycle.	Ensures enough power for all subsystem maintenance and 100% duty cycle across all four scientific instruments.
GA-POW-04	The EPS shall deliver power through a combination of solar panels and secondary batteries.	Minimizes the cost of operating power, while enabling function through solar eclipses, solar irradiance variation, and peak power cycles.
AE-POW-01	The EDL Module shall be powered solely by a primary power supply unit, maintained through cruise by the onboard radioisotope thermoelectric generator.	The EPS of AEGIS is independent such that it is not responsible for generating the power required for EDL. Batteries must remain over their end of charge voltage to prolong battery health and maintain reliability.
AE-POW-02	The EPS shall deliver enough power to support at most a 25% duty cycle for all scientific operations.	All instrumentation will be operational for 23/24 of a sol. Individual sets of instrumentation require separate running times to avoid experimental interference.
AE-POW-03	The EPS shall be capable of delivering 118.49 W in an operation power cycle.	Ensures enough power to operate scientific instrumentation, and maintain temperature.
AE-POW-04	The EPS shall be capable of delivering 256.49 W in a peak power cycle.	Ensures enough power to transmit to GALE, maintain temperatures, and remove dust from solar panels.
AE-POW-05	The EPS shall deliver power through a combination of solar panels, secondary batteries, and a radioisotope thermoelectric generator.	Minimizes the cost of operating power given the limited solar irradiance available to AEGIS during dust season.

D. Propulsion System Requirements

Table 44 Propulsion System Requirements and Rationale

ID	Requirement	Rationale
GA-PROP-01	The main propulsion unit shall produce at least 2.5 km/s of Δv .	Ensures the spacecraft has enough Δv to capture at Mars and maintain its orbit throughout the mission.
GA-PROP-02	The main propulsion unit shall produce a BOL specific impulse of at least 230 s.	Minimizes the mass of fuel required to achieve the orbital Δv requirement.
GA-PROP-03	The main propulsion unit (single thruster) shall produce a BOL thrust of at least 110 N.	Ensures the spacecraft can perform the capture maneuver quickly.
GA-PROP-04	The main propulsion unit valves shall be capable of cycling 70,000 times.	Ensures the thruster valves will not fail during the mission duration.
GA-PROP-05	The RCS propulsion unit shall produce at least 300,000 N-s of impulse.	Ensures the spacecraft can desaturate its reaction wheels frequently.
GA-PROP-06	The RCS propulsion unit shall produce a BOL specific impulse of at least 230 s.	Minimizes the mass of fuel required to achieve the orbital RCS impulse requirement.
GA-PROP-07	The RCS propulsion units (single thruster) shall produce a BOL thrust of at least 20 N.	Ensures the spacecraft can quickly desaturate its reaction wheels.
GA-PROP-08	The RCS propulsion unit valves shall be capable of cycling 100,000 times.	Ensures the thruster valves will not fail during the mission duration.
AE-PROP-01	The main propulsion unit shall produce at least 500 m/s of dV	Ensures the spacecraft has enough Δv to safely land on the Martian surface.
AE-PROP-02	The main propulsion unit shall produce a specific impulse of at least 230 s	Minimizes the mass of fuel required to achieve the landing Δv requirement.
AE-PROP-03	The main propulsion unit (single thruster) shall produce a thrust of at least 1500 N	Ensures the spacecraft can decelerate quickly enough to land softly on the Martian surface.
AE-PROP-04	The main propulsion unit valves shall be capable of cycling 70,000 times	Ensures the thruster valves will not fail during the entry, descent, and landing.
AE-PROP-05	The main propulsion system shall be able to steadily fire for 2 minutes	Ensures the propulsion system doesn't fail during the landing sequence.
AE-PROP-06	The RCS propulsion unit shall produce at least 5000 N-s of impulse	Ensures the spacecraft can maintain stability for the duration of entry.
AE-PROP-07	The RCS propulsion unit shall produce a BOL specific impulse of at least 230 s	Minimizes the mass of fuel required to achieve the landing RCS impulse requirement.
AE-PROP-08	The RCS propulsion units (single thruster) shall produce a BOL thrust of at least 20 N	Ensures the spacecraft can quickly desaturate its reaction wheels.
AE-PROP-09	The RCS propulsion unit valves shall be capable of cycling 100,000 times	Ensures the thruster valves will not fail during the entry, descent, and landing.

E. Thermal Requirements

Table 45 Thermal Control Subsystem Requirements

ID	Requirement	Rationale
OR-TCS-01	Each body shall be equipped with a thermal control system capable of maintaining all structural and within their specified operational temperature ranges under all mission phases.	Ensures survivability and performance of core space-craft systems during all mission phases
OR-TCS-02	Each scientific instrument shall be provided with an integrated thermal control system that maintains the instrument within its required operational temperature range throughout its mission timeline.	Preserves instrument functionality and protects sensitive hardware from thermal degradation
OR-TCS-03	Each thermal control subsystem shall include at least one redundant thermal management method.	Increases system robustness in the event of failure or unexpected thermal loading
AE-TCS-01	The lander's thermal protection system shall be designed to ensure thermal survivability during all phases of Entry, Descent, and Landing in accordance with predicted heating profiles.	Ensures lander integrity and instrument survival during EDL through proper thermal shielding

F. Attitude Control System Requirements

Table 46 Child-Level GALE Attitude Control System Requirements

ID	Requirement	Rationale
OR-ACS-01.01	The ACS on GALE shall use a combination of an IMU, star tracker, and sun sensors for attitude determination	Multiple instruments provide accurate data
OR-ACS-02.01	The ACS on GALE shall use its reaction wheels for primary rotational control, and the eight-22N hydrazine RCS thrusters shall be primarily reserved for desaturation and momentum dumping	Ensures reaction wheels can be desaturated properly
OR-ACS-02.02	The ACS shall desaturate GALE's reaction wheels using its RCS thrusters within 10 seconds	Ensures proper desaturation of reaction wheels can occur
OR-ACS-02.03	The ACS on GALE shall provide a maximum slew angle in all axes of at least 30 degrees per 2 minutes	Ensures quick slew maneuvers can occur
OR-ACS-02.04	The ACS shall ensure that GALE possesses a maximum pointing jitter of 5×10^{-6} milliradians	Ensures science measurements are precise and consistent
OR-ACS-02.05	The ACS shall ensure that GALE possesses a minimum pointing accuracy of 2 milliradians	Ensures science measurements are precise and consistent
OR-ACS-03.01	The ACS on GALE shall employ sensor fusion between the IMU, star tracker, and sun sensors to ensure redundancy and fault tolerance	Provides a means of redundancy to fulfill parent requirement
OR-ACS-03.02	The ACS on GALE shall possess four reaction wheels to prevent gimbal lock	Ensures full attitude control of orbiter at all times
OR-ACS-03.03	The ACS on GALE shall autonomously detect and recover from attitude control anomalies within ten seconds	Ensures quick response time in case of mishap
OR-ACS-03.04	The ACS on GALE shall be equipped with dual IMUs, sun sensors, and star trackers, to ensure redundancy	Lowers failure probability of attitude control system
GA-ACS-01.01	The ACS shall autonomously transition to safe mode if star tracker or sun sensor failure occurs	Ensures safe and lowest risk of operation in case of damage

Table 47 Child-Level AEGIS Attitude Control System Requirements

ID	Requirement	Rationale
OR-ACS-02.06	The ACS on AEGIS shall use eight 22N hydrazine RCS thrusters for full 3-axis attitude adjustments during descent	Ensures re-entry vehicle's attitude is maintained nominal
OR-ACS-03.05	The ACS on AEGIS shall use both an IMU and star tracker for navigation during Mars re-entry	Multiple instruments provide accurate data
OR-ACS-03.06	The ACS on AEGIS shall include dual IMUs, sun sensors, and star trackers for redundancy	Reduces failure probability of attitude control system
AE-ACS-01.01	The ACS shall ensure that the forebody of the re-entry vehicle is pointed towards the oncoming hypersonic/supersonic flow to maintain TPS effectiveness	Ensures thermal protection system (TPS) effectiveness
AE-ACS-01.02	The ACS shall autonomously detect and compensate for Mars wind effects to ensure controlled landing	Provides effective autonomous guidance
AE-ACS-04.01	The ACS shall use three onboard inclinometers to monitor lander tilt and actuate its adjustable legs if needed	Ensures lander maintains its appropriate orientation

G. Communications Requirements

Table 48 Communications Subsystem Requirements

ID	Requirement	Rationale
GA-COMM-01	The communication subsystem shall be capable of a 1.22 Kbps CTR	there is 63.3 Gb of data acquired in a day with on average 75% of time Line of Sight to Earth
GA-COMM-02	The communication subsystem shall be capable of a pointing accuracy of 10 mrad	Ensures pointing losses are small and full earth coverage
GA-COMM-03	The communication subsystem shall be capable of communicating in the X-band frequency range with the Deep Space Network	Using DSN for communication
GA-COMM-03.01	The communication subsystem shall be tested in an anechoic chamber to confirm frequency and gain during operation	Validation Requirement
GA-COMM-04	The communication subsystem shall be capable of storing 550 Gb of data	Storage for up to one week of data acquisition
GA-COMM-05	The communication subsystem shall have a bit error rate of less than E-5	SNR of 10 dB
GA-COMM-06	The communication subsystem shall operate with a base plate temperature of at least -35 C and at most 80 C	Ensures frequency stability and gains within margin
GA-COMM-06.01	The communication system shall be tested in an environmental chamber at -35 C, 25 C and 80 C to ensure specifications are met	Validation Requirement
AE-COMM-01	The communication subsystem shall be capable of a 7.35 Mbps CTR	There is 4.6 Gb of data acquired in a day, with approximately 16 minutes of ground passes in a day
AE-COMM-02	The communication subsystem shall be capable of pointing an antenna to track the GALE orbiter during ground passes	Since the orbiter is moving, in order to send telemetry the antenna must be able to track the moving satellite
AE-COMM-03	The communication subsystem shall be capable of communication in the UHF frequency range	Lower frequencies provide reliable signal strength and penetration in the case of dust storms
AE-COMM-03.01	The communication subsystem shall be tested in an anechoic chamber to confirm frequency and gain during operation	Validation Requirement
AE-COMM-04	The communication subsystem shall be capable of storing at least 14.12 Gb of data	Storage for up to two days of data acquisition
AE-COMM-05	The communication subsystem shall have a bit error rate of less than E-5	SNR of 10 dB
AE-COMM-06	The communication subsystem shall operate with a base plate temperature of at least -20 C and at most 70 C	Ensures frequency stability and gains within margin
AE-COMM-06.01	The communication system shall be tested in an environmental chamber at -20 C, 25 C and 70 C to ensure specifications are met	Validation Requirement

H. Payloads Requirements

Table 49 Scientific Instrumentation Requirements and Rationale

ID	Requirement	Rationale
GA-INSTR-01	The Doppler aerosol wind lidar shall record Martian aeolian activity through observing Rayleigh and Mie Scattering.	Understanding Martian wind patterns is essential for studying dust storms, erosion, and atmospheric dynamics, which influence climate models and future exploration.
GA-INSTR-02	The reconnaissance imaging spectrometer shall record infrared activity related to Martian atmospheric activity.	Infrared imaging allows for studying temperature variations, atmospheric composition, and seasonal changes in the Martian atmosphere.
GA-INSTR-03	The infrared radiometer shall record thermal and inertial maps as a function of Mars atmospheric altitude.	Thermal and inertial data are crucial for analyzing surface heat retention, atmospheric density variations, and potential landing site selection.
GA-INSTR-04	The subsurface radar sounder shall record the presence of water ice and lava tubes for human exploration on Hellas Planitia.	Detecting water ice is essential for in-situ resource utilization, while lava tubes could serve as natural shelters for future human missions.
AE-INSTR-01	The saltation sensor, dust anemometer, and imaging cameras shall record the movement of dust particles and sediment while operating in Hellas Planitia.	Understanding dust movement and sediment transport helps predict dust storm behavior, which impacts lander operations and solar power efficiency.
AE-INSTR-02	The radiation assessment detector and flux radiometer shall record energy distributions from high-energy particles while operating in Hellas Planitia.	Measuring radiation exposure is critical for assessing risks to future human explorers and sensitive electronic components.
AE-INSTR-03	The thermocouples, pressure transducer, electric field sensor, and wind sensor shall record general Martian environmental conditions while operating in Hellas Planitia.	Environmental data provides insight into Martian weather patterns, atmospheric pressure fluctuations, and surface interactions affecting mission success.
AE-INSTR-04	The radar Doppler altimeter shall record the altitude of the lander during AEGIS' descent into Mars.	Accurate altitude data ensures precise landing operations and contributes to terrain-relative navigation systems for future missions.
AE-INSTR-05	The aerothermal sensors and descent camera shall document Martian atmospheric conditions during AEGIS' descent into Mars.	Understanding aerothermal effects and atmospheric density variations supports future entry, descent, and landing (EDL) system designs.

References

- [1] National Aeronautics and Space Administration (NASA), “Moon to Mars Strategy and Objectives Development,” , 2023.
- [2] Rennie, M. P., “An assessment of the expected quality of Aeolus Level-2B wind products,” *EPJ Web of Conferences*, Vol. 176, 2018, p. 02015. <https://doi.org/10.1051/epjconf/201817602015>.
- [3] Seiff, A., and Kirk, D. B., “Structure of the atmosphere of Mars in summer at mid-latitudes,” *Journal of Geophysical Research*, Vol. 82, No. 28, 1977, p. 4364–4378. <https://doi.org/10.1029/JS082i028p04364>.
- [4] NASA Ames Research Center, “Trajectory Browser,” <https://trajbrowser.arc.nasa.gov>, 2025.
- [5] Malyuta, D., “Convex Optimization for Trajectory Generation: A Tutorial on Generating Dynamically Feasible Trajectories Reliably and Efficiently,” *IEEE Control Systems Magazine*, Vol. 42, No. 5, 2022, pp. 40–71. <https://doi.org/10.1109/MCS.2022.3187542>.
- [6] Team, S. F. E., “Aerojet Rocketdyne Propulsion to Enable NASA Perseverance Rover’s Landing on Mars,” *Space Foundation Partner News*, 2021. URL <https://www.spacefoundation.org/2021/02/18/aerojet-rocketdyne-propulsion-to-enable-nasa-perseverance-rovers-landing-on-mars/>.
- [7] Jet Propulsion Laboratory, C. I. o. T., *DSN Radio Astronomy Users Guide*, 2023. URL https://deepspace.jpl.nasa.gov/files/DSN_Radio_Astronomy_Users_Guide.pdf, accessed: 2025-03-07.
- [8] Jet Propulsion Laboratory, C. I. o. T., *NASA’s Mission Operations and Communications Services*, 2014. URL https://deepspace.jpl.nasa.gov/files/6_NASA_MOCS_2014_10_01_14.pdf, accessed: 2025-03-07.
- [9] Abshire, J. B., Smith, M. D., Cremons, D. R., Guzewich, S. D., Sun, X., Yu, A., and Hovis, F., “MARLI: MARS LIDAR FOR MEASURING GLOBAL WIND AND AEROSOL PROFILES FROM ORBIT,” April 7, 2022.
- [10] Bedka, K. M., Nehrir, A. R., Kavaya, M., Barton-Grimley, R., Beaubien, M., Carroll, B., Collins, J., and Cooney, J., “Airborne lidar observations of wind, water vapor, and aerosol profiles during the NASA Aeolus calibration and validation (Cal/Val) test flight campaign,” *Atmospheric Measurement Techniques*, Vol. 14, No. 6, 2021, p. 4305–4334. <https://doi.org/10.5194/amt-14-4305-2021>.
- [11] Bell, J. F., Maki, J. N., Mehall, G. L., Ravine, M. A., Caplinger, M. A., Bailey, Z. J., Brylow, S., Schaffner, J. A., and Kinch, K. M., “The Mars 2020 Perseverance Rover Mast Camera Zoom (Mastcam-Z) Multispectral, Stereoscopic Imaging Investigation,” *Space Science Reviews*, Vol. 217, No. 1, 2021, p. 24. <https://doi.org/10.1007/s11214-020-00755-x>.
- [12] Bettanini, C., Esposito, F., Debei, S., Molfese, C., Rodriguez, I. A., Colombatti, G., Harri, A.-M., and Montmessin, F., “The DREAMS experiment on the ExoMars 2016 mission for the study of Martian environment during the dust storm season,” *2014 IEEE Metrology for Aerospace (MetroAeroSpace)*, IEEE, Benevento, Italy, 2014, p. 167–173. <https://doi.org/10.1109/MetroAeroSpace.2014.6865914>, URL <http://ieeexplore.ieee.org/document/6865914/>.

- [13] Committee on the Planetary Science and Astrobiology Decadal Survey and Space Studies Board and Division on Engineering and Physical Sciences and National Academies of Sciences, Engineering, and Medicine, *Origins, Worlds, and Life: Planetary Science and Astrobiology in the Next Decade*, National Academies Press, Washington, D.C., 2023. <https://doi.org/10.17226/27209>, URL <https://www.nap.edu/catalog/27209>.
- [14] Esposito, F., Debei, S., Bettanini, C., Molfese, C., Arruego Rodríguez, I., Colombatti, G., Harri, A.-M., and Montmessin, F., “The DREAMS Experiment Onboard the Schiaparelli Module of the ExoMars 2016 Mission: Design, Performances and Expected Results,” *Space Science Reviews*, Vol. 214, No. 6, 2018, p. 103. <https://doi.org/10.1007/s11214-018-0535-0>.
- [15] Ferri, F., Fulchignoni, M., Colombatti, G., Stoppato, P. F. L., Zarnecki, J. C., Harri, A. M., Schwingenschuh, K., Hamelin, M., Flaminii, E., Bianchini, G., and Angrilli, F., “THE HUYGENS ATMOSPHERIC STRUCTURE INSTRUMENT (HASI): EXPECTED RESULTS AT TITAN AND PERFORMANCE VERIFICATION IN TERRESTRIAL ATMOSPHERE,” 2005.
- [16] Gülan, A., Thiele, T., Siebe, F., and Kronen, R., “Combined Instrumentation Package COMARS+ for the ExoMars Schiaparelli Lander,” *Space Science Reviews*, Vol. 214, No. 1, 2018, p. 12. <https://doi.org/10.1007/s11214-017-0447-4>.
- [17] Greer, L., and Krasowski, M., “A Saltation Sensor for the Martian Aqueous Habitat Reconnaissance Suite (MAHRS),” 2021.
- [18] Karlgaard, C. D., Korzun, A. M., Schoenenberger, M., Bonfiglio, E. P., Kass, D. M., and Grover, M. R., “Mars InSight Entry, Descent, and Landing Trajectory and Atmosphere Reconstruction,” 2020.
- [19] Lipatov, A. N., Ekonomov, A. P., Makarov, V. S., Lesnykh, V. A., Goretov, V. A., Zakharkin, G. V., Zaitsev, M. A., Khlyustova, L. I., and Antonenko, S. A., “Accelerometers of the Meteorological Complex for the Study of the Upper Atmosphere of Mars,” *Solar System Research*, Vol. 57, No. 4, 2023, p. 349–357. <https://doi.org/10.1134/S0038094623040081>.
- [20] Lipatov, A. N., Lyash, A. N., Ekonomov, A. P., Makarov, V. S., Lesnykh, V. A., Goretov, V. A., Zakharkin, G. V., Khlyustova, L. I., Antonenko, S. A., Rodionov, D. S., and Koralev, O. I., “LIDAR for Investigation of the Martian Atmosphere from the Surface,” *Solar System Research*, Vol. 57, No. 4, 2023, p. 358–372. <https://doi.org/10.1134/S0038094623040093>.
- [21] Montmessin, F., Déprez, G., Vivat, F., Hassen-Kodja, R., Granier, P., and Lapauw, L., “THE MICRO-ARES EXPERIMENT AS PART OF THE DREAMS METEOROLOGICAL SUITE ONBOARD SCHIAPARELLI: A PROMISE AND A DEMISE,” 2017.
- [22] Moore, J. M., and Edgett, K. S., “Hellas Planitia, Mars: Site of net dust erosion and implications for the nature of basin floor deposits,” *Geophysical Research Letters*, Vol. 20, No. 15, 1993, p. 1599–1602. <https://doi.org/10.1029/93GL01302>.
- [23] Petrosyan, A., Galperin, B., Larsen, S. E., Lewis, S. R., Määttänen, A., Read, P. L., Renno, N., Rogberg, L. P. H. T., Savijärvi, H., Siili, T., Spiga, A., Toigo, A., and Vázquez, L., “THE MARTIAN ATMOSPHERIC BOUNDARY LAYER,” *Reviews of Geophysics*, Vol. 49, No. 3, 2011, p. 2010RG000351. <https://doi.org/10.1029/2010RG000351>.
- [24] Schweizer, C., Mashuga, C. V., and Kulatilaka, W. D., “Investigation of aluminum dust cloud dispersion characteristics in an explosion hazard testing device using laser-based particle and flow diagnostics,” *Process Safety and Environmental Protection*, Vol. 166, 2022, p. 310–319. <https://doi.org/10.1016/j.psep.2022.08.013>.

- [25] Shipley, S. T., Tracy, D. H., Eloranta, E. W., Trauger, J. T., Sroga, J. T., Roesler, F. L., and Weinman, J. A., “High spectral resolution lidar to measure optical scattering properties of atmospheric aerosols 1: Theory and instrumentation,” *Applied Optics*, Vol. 22, No. 23, 1983, p. 3716. <https://doi.org/10.1364/AO.22.003716>.
- [26] Vago, J. L., Coates, A. J., Jaumann, R., Koralev, O., Ciarletti, V., Mitrofanov, I., Josset, J.-L., Westall, F., and Team, T. E., *Searching for Traces of Life With the ExoMars Rover*, Elsevier, 2018, p. 309–347. <https://doi.org/10.1016/B978-0-12-809935-3.00011-6>, URL <https://linkinghub.elsevier.com/retrieve/pii/B9780128099353000116>.
- [27] Zakharov, A. V., Dolnikov, G. G., Kuznetsov, I. A., Lyash, A. N., Esposito, F., Molfese, C., Rodríguez, I. A., Seran, E., and Godefroy, M., “Dust Complex for Studying the Dust Particle Dynamics in the Near-Surface Atmosphere of Mars,” *Solar System Research*, Vol. 56, No. 6, 2022, p. 351–368. <https://doi.org/10.1134/S0038094622060065>.
- [28] Zeitlin, C., Hassler, D. M., Wimmer-Schweingruber, R. F., Ehresmann, B., Appel, J., Berger, T., Böhm, E., Böttcher, S., and Brinza, D. E., “Calibration and Characterization of the Radiation Assessment Detector (RAD) on Curiosity,” *Space Science Reviews*, Vol. 201, No. 1–4, 2016, p. 201–233. <https://doi.org/10.1007/s11214-016-0303-y>.
- [29] Gurnett, D. A., Green, J. L., Persoon, A. M., Morgan, D. A., Duru, F., and Nielsen, E., “The Mars Express MARSIS Sounder Instrument,” *Planetary and Space Science*, 2009. URL https://space.physics.uiowa.edu/~dag/publications/2009_TheMarsExpressMARSISSounderInstrument_PSS.pdf.
- [30] Mehta, J., “Mars Pathfinder, the start of modern Mars exploration,” *The Planetary Society*, 2022.
- [31] Millour, E. e. a., “Mars Climate Database,” Europlanet Science Congress, 2022. Version 6.1.
- [32] NASA, “InSight Lander,” NASA, 2022.
- [33] “Here’s How Curiosity’s Sky Crane Changed the Way NASA Explores Mars,” 2024.
- [34] Ball, A. J., Blancquaert, T., Bayle, O., Lorenzoni, L. V., Haldemann, A. F. C., and the Schiaparelli EDM team, “The ExoMars Schiaparelli Entry, Descent and Landing Demonstrator Module (EDM) System Design,” *Space Science Reviews*, Vol. 218, No. 5, 2022, p. 44. <https://doi.org/10.1007/s11214-022-00898-z>.
- [35] Bettanini, C., Esposito, F., Debei, S., Molfese, C., Rodriguez, I. A., Colombatti, G., Harri, A.-M., and Montmessin, F., “The DREAMS experiment on the ExoMars 2016 mission for the study of Martian environment during the dust storm season,” *2014 IEEE Metrology for Aerospace (MetroAeroSpace)*, IEEE, Benevento, Italy, 2014, p. 167–173. <https://doi.org/10.1109/MetroAeroSpace.2014.6865914>, URL <http://ieeexplore.ieee.org/document/6865914/>.
- [36] Kokubo, E., and Genda, H., “Formation of Terrestrial Planets from Protoplanets under a Realistic Accretion Condition,” *The Astrophysical Journal*, Vol. 714, No. 1, 2010, p. L21–L25. <https://doi.org/10.1088/2041-8205/714/1/L21>, arXiv:1003.4384 [astro-ph].
- [37] Levine, J. S., Kraemer, D. R., and Kuhn, W. R., “Solar radiation incident on Mars and the outer planets: Latitudinal, seasonal, and atmospheric effects,” *Icarus*, Vol. 31, No. 1, 1977, p. 136–145. [https://doi.org/10.1016/0019-1035\(77\)90076-8](https://doi.org/10.1016/0019-1035(77)90076-8).

- [38] Pappa, R. S., Rose, G., Chamberlain, M. K., Paddock, D., and Mikulas, M., “Compact Telescoping Surface Array for Mars Solar Power,” *2018 AIAA Spacecraft Structures Conference*, American Institute of Aeronautics and Astronautics, Kissimmee, Florida, 2018. <https://doi.org/10.2514/6.2018-1944>, URL <https://arc.aiaa.org/doi/10.2514/6.2018-1944>.